



Project FORTE - Nuclear Thermal Hydraulics Research & Development

**University of Manchester Research on the
Aerosol-Laden Argon Cover Gas Region above
the Sodium Pool of an LMFB**



August 2019

FNC 53798/48652R Issue 1

SYSTEMS AND ENGINEERING TECHNOLOGY

An introduction to Project FORTE

The Department for Business, Energy and Industrial Strategy (BEIS) has tasked Frazer-Nash Consultancy and its partner organisations to deliver the first phase of a programme of nuclear thermal hydraulics research and development.

Phase 1 of the programme comprises two parts:

- ▶ The specification and development of innovative thermal hydraulic modelling methods and tools; and
- ▶ The specification of a new United Kingdom thermal hydraulics test facility.

The work is intended to consider all future reactor technologies including Gen III+, small modular reactors and advanced reactor technologies.

Our project partners

The team is led by Frazer-Nash Consultancy and includes:



The
University
Of
Sheffield.



Westinghouse



The University of Manchester



**Science & Technology
Facilities Council**

For more information, visit www.innovationfornuclear.co.uk/nuclearthermalhydraulics.html

Executive Summary

Research at the University of Manchester on aspects of heat transfer from the pool of a sodium-cooled fast reactor across the aerosol-laden argon cover gas to the reactor roof began in 1980. It started in response to a request from the UKAEA for help in measuring the emissivity of a liquid sodium pool surface and was followed by an ongoing programme of sponsored research funded by the UKAEA and NNC Limited. This research continued until 1993 when the British Government ceased to fund Liquid Metal Fast Breeder Reactor (LMFBR) development in the UK.

This report covers experimental measurements at the University of Manchester on the emissivity of surfaces relevant to sodium-cooled fast reactors and heat transfer across the aerosol-laden cover gas. The experimental tests and results from this research are summarised in this report.

Surface emissivity measurements

- ▶ The emissivity, ε of liquid sodium was measured in a bespoke test facility for a range of temperatures from 300°C ($\varepsilon=0.024$) to 600°C ($\varepsilon=0.04$). Some enhancement of the emissivity was measured when ripples were generated on the surface of liquid sodium.
- ▶ The emissivity of stainless steel was measured for a range of surface finishes, treatments and emittance directions. The total hemispherical values varied from 0.15 for polished specimens to 0.6 depending on the surface finish and treatment.
- ▶ A glove box test facility was designed and built to measure the emissivity of stainless steel with filmwise and dropwise condensation of liquid sodium on the surface. The emissivity for filmwise condensation was consistent with the liquid sodium values, while dropwise condensation increased the emissivity but was sensitive to surface temperature.
- ▶ The impact on emissivity of single and repeated dryout of filmwise condensation of liquid sodium on a stainless surface was also investigated. Prior to dryout, the emissivity was consistent with the pure liquid sodium values, after which it rose to 0.4 (1 cycle) and 0.9 (7-8 cycles) during and after dryout due to chemical reactions at the high temperatures achieved.

Aerosol-laden cover gas heat transfer

- ▶ The Manchester University Sodium Aerosol Characteristics (MUSAC) large scale sodium pool test facility with a 780 mm diameter sodium pool was commissioned in 1989. This was used to investigate aerosol size distribution and concentration in the argon cover gas region, the cover gas temperature distribution and rate of sodium deposition on the side wall.
- ▶ The test section was a cylindrical vessel of 800 mm diameter and height of 320 mm at the shallow end and 390 mm at the deep end. The pool and roof of the test section were set to fixed temperatures, while the side wall was maintained at the average cover gas temperature. Instrumentation included fixed and moveable thermocouple combs, roof thermocouples, a Malvern Instrument, a Jet Impactor for making aerosol size and concentration measurements and heat flux meters for making measurements of heat transfer through the roof.
- ▶ Over the range of experimental conditions covered in the experiments, the cover gas space was well mixed. Consequently, the bulk of the cover gas space was at a uniform temperature and the sodium aerosol characteristics were uniform. The sodium aerosol concentration seemed to be mainly controlled by the liquid sodium pool temperature (300°C to 550°C), while the roof temperature (120°C to 200°C) did not appear to have any systematic influence.
- ▶ The pool temperature had a stronger influence on the aerosol mean diameter than the roof temperature. The higher the pool temperature, the larger was the mean aerosol diameter. The rate of heat transfer to the roof increased monotonically with increase of the sodium pool temperature for fixed roof temperature, while changing the roof temperature had little effect on the rate of heat transfer to the roof for a fixed pool sodium temperature.

Contents

1	BACKGROUND	5
2	LIQUID SODIUM EMISSIVITY MEASUREMENTS	6
3	STAINLESS STEEL EMISSIVITY MEASUREMENTS	8
4	IMPACT OF SODIUM CONTAMINATION ON EMISSIVITY	11
4.1	Initial Measurements Using a Simple Glove Box Test Facility	11
4.2	An Improved Glove Box Test Facility	12
5	STUDIES OF SODIUM CONDENSATION	16
6	IMPACT OF RIPPLES ON EMISSIVITY	18
7	IMPACT OF DROPWISE CONDENSATION ON EMISSIVITY	20
8	IMPACT OF EVAPORATION AND DRYOUT ON EMISSIVITY	24
8.1	Single Dryout of a Sodium Film	24
8.2	Repeated Dryout of Sodium Filmwise Condensation	25
9	THE MUSAC RESEARCH PROJECT	28
9.1	Preliminary Studies of the Sodium Aerosol Cloud	28
9.2	Description of a Large Scale Sodium Pool Test Facility (MUSAC)	29
9.3	Commissioning Tests	31
9.4	Initial Programme of Experimental Work on the MUSAC Test Facility	31
9.5	Results from the Initial Programme of Experimental Work	32
9.6	Further Experimental Studies	38
9.7	Conclusions	46
10	REFERENCES	47

1 Background

An active interest in Liquid Metal Fast Breeder Reactors (LMFBRs) developed in Britain during the nineteen fifties led in the first instance to the design, construction and operation by the United Kingdom Atomic Energy Authority (UKAEA) of the Dounreay Fast Reactor (DFR), a relatively small sodium-cooled loop-type system. This was followed in the nineteen sixties and seventies by the design, construction and operation at Dounreay of the 200 MWe pool type Prototype Fast Reactor (PFR).

The UKAEA then began work on the design of a Commercial Development sodium-cooled Fast Reactor (CDFR). Information was needed concerning heat transfer across the cover gas space between the sodium pool and the roof in order to determine the amount of roof insulation and the forced convection cooling needed. In 1979, the UKAEA approached Manchester University with a view to carrying out research in the Nuclear Engineering Laboratory there to measure the emissivity of liquid sodium under fast reactor temperature conditions. Thus, in 1980, a programme of research led by Professor J.D. Jackson was initiated there on that topic.

Subsequently, the UKAEA and NNC Limited funded an ongoing series of further experimental investigations at Manchester University aimed at providing information concerning heat transfer across the sodium aerosol laden argon cover gas region above a sodium pool. This provided valuable results which were used by the UKAEA and NNC Limited, in the course of the UK contribution to the European Fast Reactor (EFR) Development Programme. However, in 1993, the research came to an abrupt end when the UK Government decided to terminate all work in the UK on LMFBRs and withdrew from the EFR Research Programme. This report outlines the research carried out at Manchester University on that topic from 1980 to 1993.

2 Liquid Sodium Emissivity Measurements

This challenging experimental study was carried out over a period of three years by a PhD student, D.K.W. Tong [1] under the supervision of Professor Jackson. In 1980, work began on the design and construction of a test facility to measure the emittance of thermal radiation from the free surface of a slowly overflowing pool of sodium. An outline of the test facility is shown in Figure 1, and a schematic diagram of the test section arrangement is shown in Figure 2.

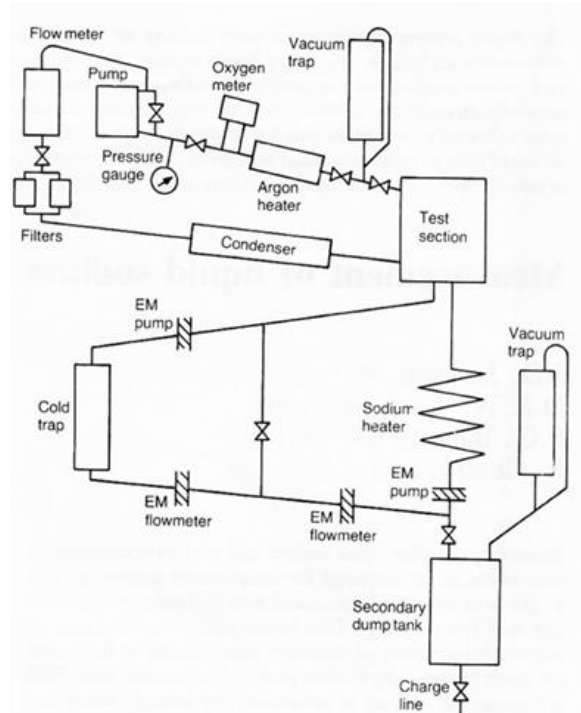


Figure 1: The sodium pool emittance test facility

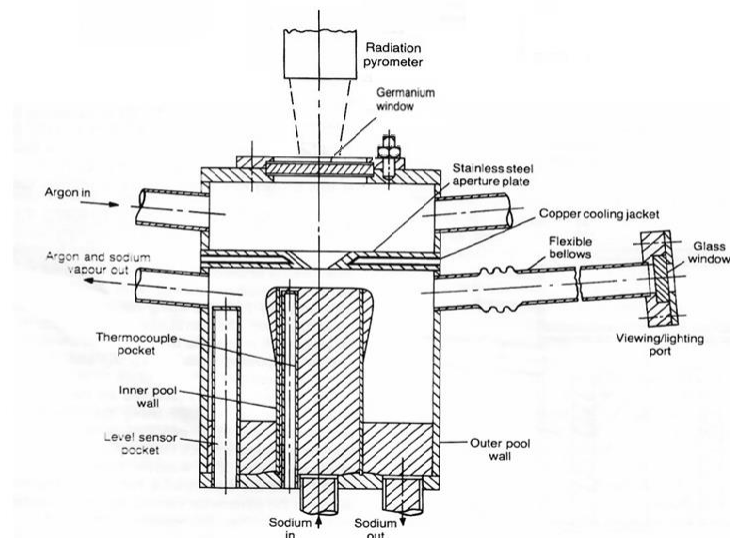


Figure 2: Schematic of the test section

The sodium pool surface, was carefully purged from above by a slow flow of argon gas to remove any sodium aerosol cloud which otherwise would have been present above it. This was done without disturbing the free surface of the sodium pool. The free surface could then be viewed from above by a carefully calibrated high precision radiation pyrometer through a germanium window and an orifice plate. Thus, the emission of thermal radiation from the sodium pool surface in the normal direction could be determined after making suitable corrections for the ambient radiation reflected from the pool surface received by the pyrometer, taking account of the measured transmissivity of the germanium window. The flows of clean argon gas and liquid sodium, respectively, were provided by closed loop circuits, each incorporating sodium clean-up systems.

The research began with development work on measurements using the radiation pyrometer of the total normal emissivity of a number of specularly reflective specimens of stainless steel, copper, aluminium and liquid tin. The pyrometer had been carefully calibrated beforehand using a standard Black Body reference source. This enabled experimental techniques to be developed for use later in the proposed liquid sodium emissivity measurements.

The sodium pool test section arrangement was designed, manufactured and commissioned, along with the associated argon and sodium flow circuits. Experiments then began to obtain the required sodium pool emittance data. By 1983 some very reliable and accurate measurements had been made of liquid sodium emissivity covering a range of sodium pool temperatures from 300°C to 600°C. These were correlated as a function of pool temperature using a simple linear regression analysis.

The following equation was found to fit the measured variation of total normal emissivity, E_s , of liquid sodium with temperature, T_s (in degree Centigrade), to an accuracy better than 10%.

$$E_s = 0.00775 + 0.0000541 T_s \quad (1)$$

These were the first reliable measurements of liquid sodium emissivity ever to be reported.

3 Stainless Steel Emissivity Measurements

The investigation of thermal radiation from the surface of a liquid sodium pool had involved some preliminary development work using specularly reflective stainless steel surfaces. In the course of this research, the UKAEA decided to broaden the scope of the work at Manchester University to include some detailed measurements of the emissivity of stainless steel and mild steel. In 1981, a further PhD student, E. Romero [2] was recruited and commenced work on this topic. He covered a wide range of surface conditions, measuring not only the emittance of thermal radiation normal to a surface but also the directional values.

As can be seen from Figure 3(a), a feature of the measured directional emissivity of electro-polished stainless steel was that it increased with angle, slowly at first but then quite rapidly at angles above 70°, achieving a value of over twice the normal value, at an angle of 85°. Figure 3(b) shows integrated hemispherical values as a function of temperature.

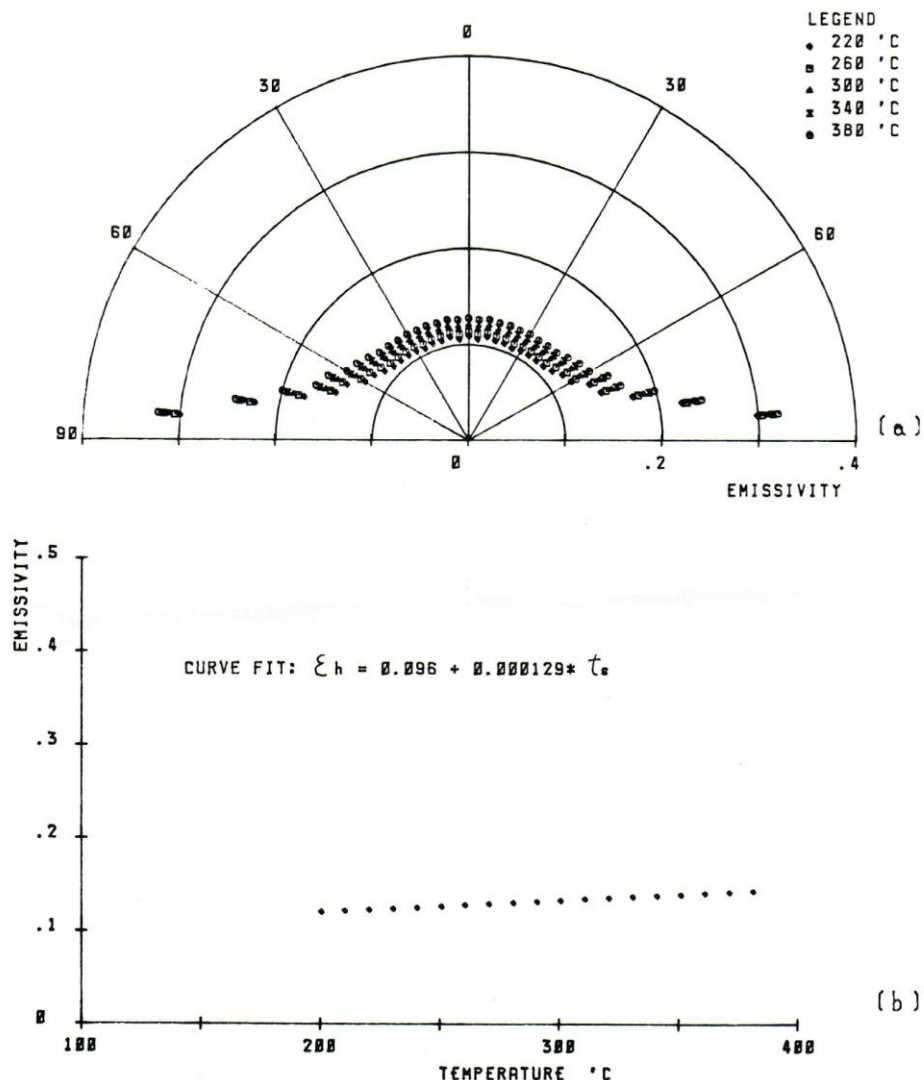


Figure 3: Emissivity of electro-polished stainless steel
(a) Directional Emissivity, (b) Integrated Hemispherical Emissivity

It was found that the emissivity of a smooth polished stainless steel specimen could be increased very readily by heat treatment (oxidisation). Its emissivity changed from 0.15 to about 0.4 by heating it up in air to a temperature of about 750°C. This caused it to become a diffuse emitter, as shown in Figure 4.

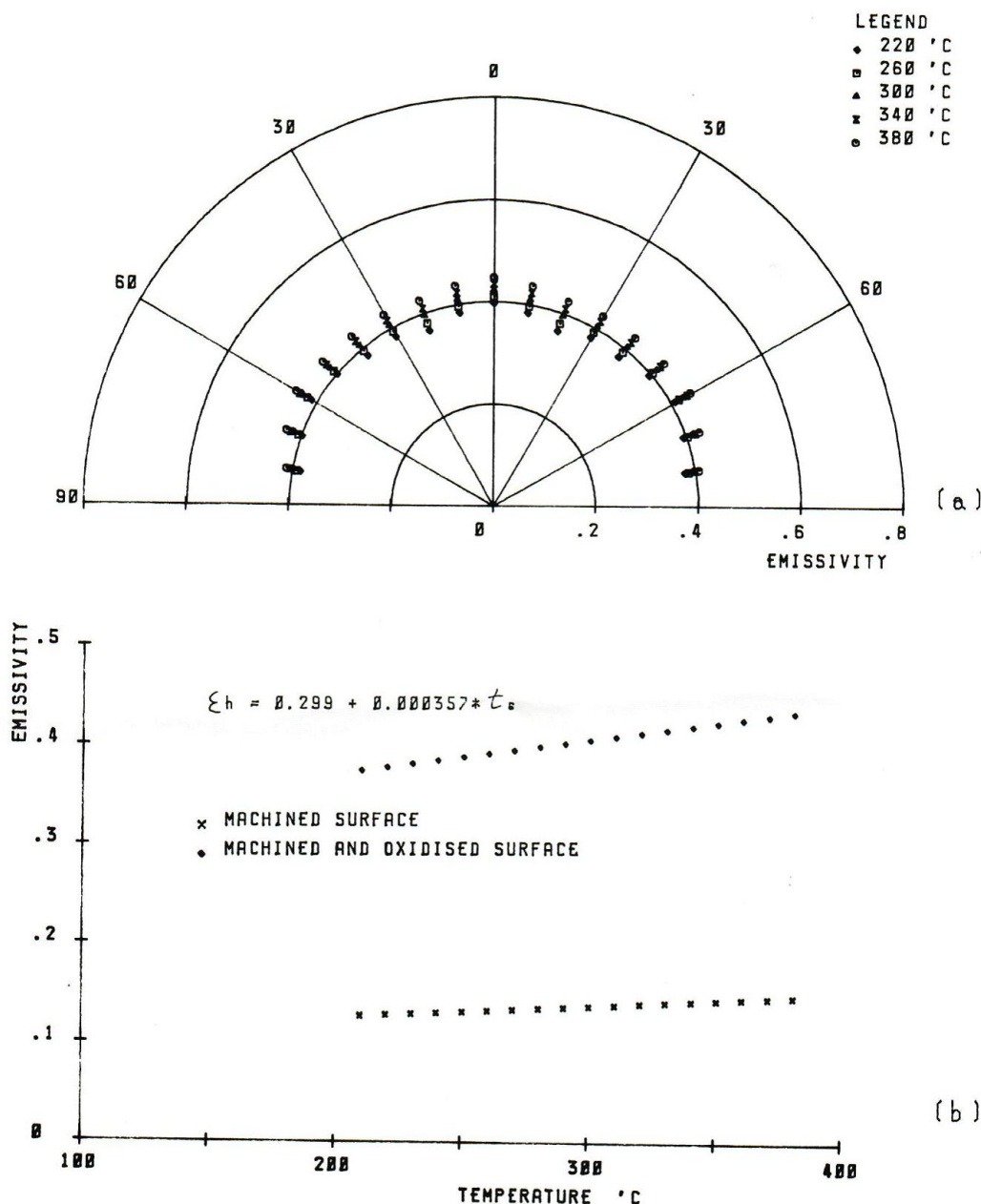


Figure 4: Machined and oxidised stainless steel
(a) Directional Emissivity, (b) Integrated Hemispherical Emissivity

Polished stainless steel raised to temperatures up to 1100°C in a Nitrogen atmosphere (nitriding) had a high value of emissivity (about 0.6). The emissivity of polished stainless steel could also be readily increased by chemical action. Using an aqueous solution of potassium chromate and sulphuric acid at a temperature of about 95°C the emissivity of a stainless steel surface could be increased to about 0.6. Oxide layers, produced in the course of the manufacture of stainless steel caused the emissivity of 'as received' specimens to vary

significantly. They were found to have values which ranged from about 0.2 to 0.6 depending on the manufacturing process (see Romero [2]).

The emissivity of mild steel in a clean bright machined state was found to be even lower than that of polished stainless steel, but its value increased very readily to over 0.5 by heating it up in air to a temperature of only 300°C. In its 'as received' state with a dark grey scale on its surface, the emissivity of mild steel was over 0.4. Grit blasting a machined mild steel specimen increased its emissivity to about 0.4. If this was followed by heat treatment, values of about 0.7 were readily achieved. When treated with salt solution the emissivity of mild steel increased to over 0.6.

Values of emissivity over 0.9 were achieved by coating steel surfaces with a proprietary black paint, 'Nextel'. However, this had the drawback that it deteriorated at temperatures above 300°C. 'Sperex' was an alternative high emissivity paint, which had an emissivity of about 0.8 and could stand much higher temperatures (up to about 600°C).

4 Impact of Sodium Contamination on Emissivity

4.1 Initial Measurements Using a Simple Glove Box Test Facility

In 1982, an experimental study was initiated to measure the emissivity of sodium contaminated stainless steel surfaces i.e. the stainless steel surface has been in contact with liquid sodium at a high temperature e.g. 400°C. This was carried out by an MSc student, L. Iravanian [3], who designed and constructed a glove box test facility for measuring the emissivity of sodium contaminated specimens in an argon environment (see Figure 5).

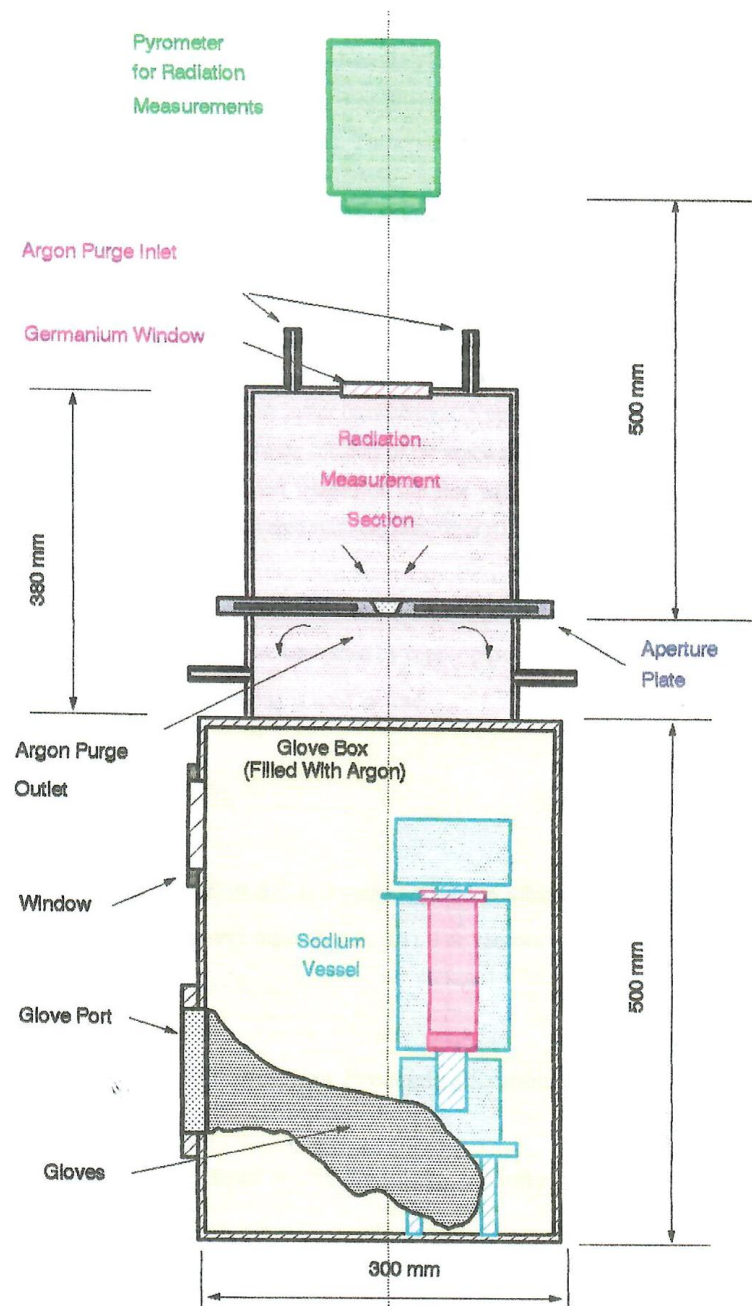


Figure 5: Schematic of the initial glove box test facility

The thermal radiation measurement section on top of the glove box, was similar to that developed earlier by Tong [1]. Clean argon was supplied to the radiation measurement section and the glove box from a closed circuit flow loop incorporating a simple argon clean-up system.

Machined and electro-polished specimens of Type 316 stainless steel were prepared and sent to the UKAEA Risley Laboratories for immersion in flowing liquid sodium at 450°C for a period of 13 weeks. They were then vacuum distilled at a temperature of 350°C before being returned to the University of Manchester and loaded into the glove box. Then, one by one, the specimens were transferred to the thermal radiation measurement section and tested.

In the course of these experiments it was found that the contamination of the specimens by liquid sodium at 450°C had led to significantly increased emissivity. In the test shown on Figure 6, the emissivity of the specimen was initially about 0.45. At a temperature of about 300°C, the emissivity increased, slowly at first but at a greater and greater rate, reaching a peak value of just over 0.8 at a temperature of under 500°C. After this, the emissivity remained more or less constant with further increase of temperature up to 580°C. On cooling down it remained at a high value of about 0.8.

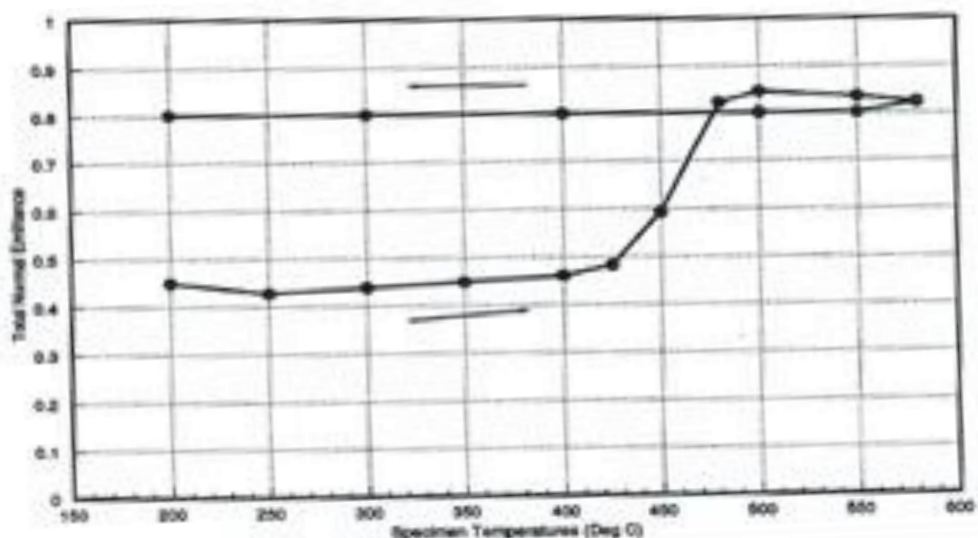


Figure 6: Total normal emittance of a sodium contaminated stainless steel specimen

It was decided that small traces of air present in the argon gas supplied to the test facility were responsible for this irreversible behaviour. Clearly, an improved version of the glove box test facility was needed before proceeding with any further work of this kind.

4.2 An Improved Glove Box Test Facility

A further Ph.D student, K.L.A. Lam [4], was recruited and he began by designing and developing a closed circuit clean-up system capable of continuously delivering argon of very high purity to both the glove box and the thermal radiation measurement section. Figure 7 shows the complete arrangement (see also Plate 1).

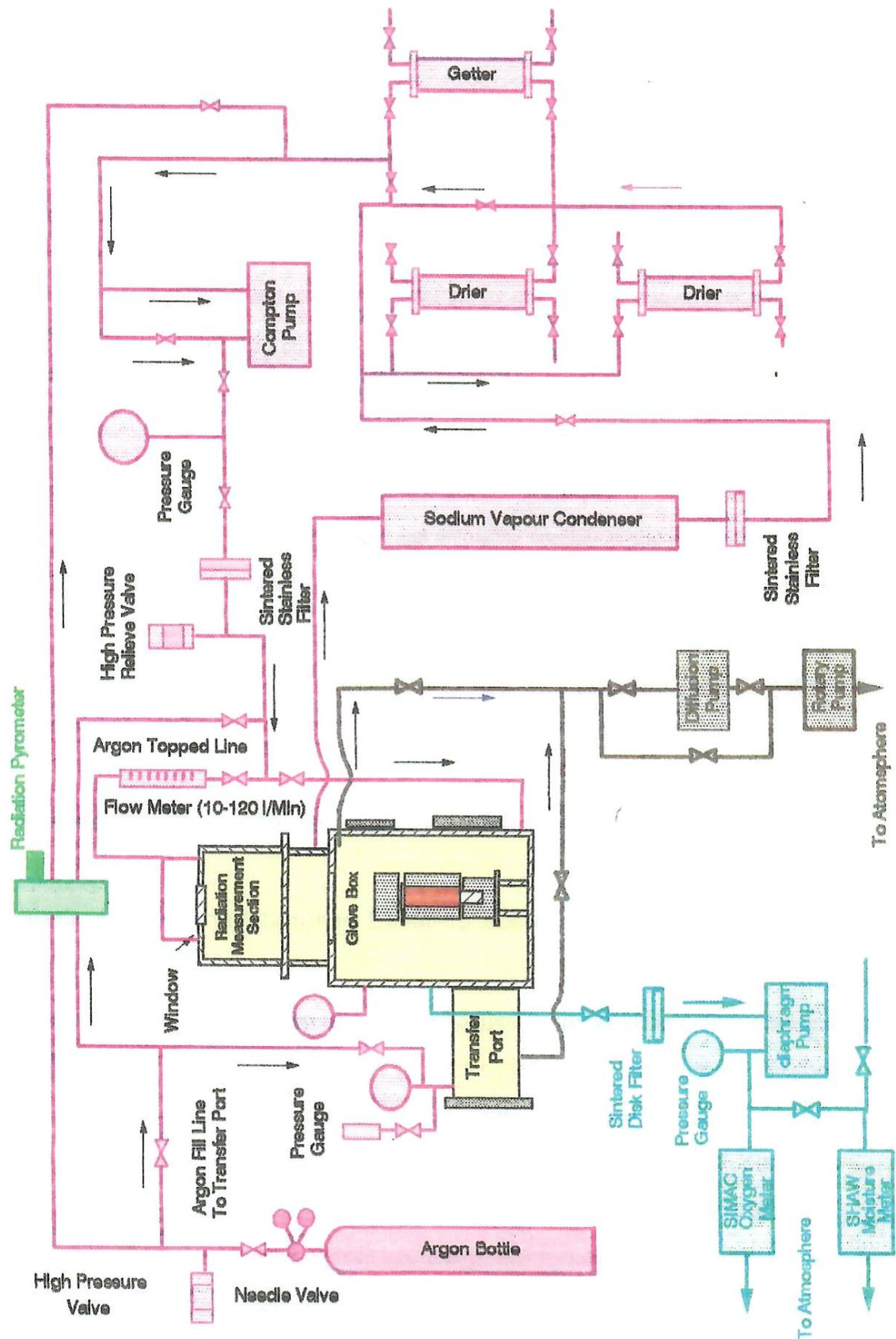


Figure 7: General arrangement of the improved glove box test facility



Plate 1: Photograph of the improved glove box test facility

Lam [4] then carried out experiments using the improved test facility to demonstrate that it could be used for measuring the emissivity of the surface of a shallow pool of liquid sodium in a recess of depth 2 mm and diameter 17mm on a stainless steel disc mounted on a heater block.

- ▶ An empty disc was heated up to 300°C in the glove box and then clean reactor grade sodium was melted in the recess so as to fill it with liquid sodium.
- ▶ The heater and sodium-filled specimen were then transferred from the glove box into the Thermal Radiation Measurement Test Section.
- ▶ There, the pool of sodium was heated up slowly from 200°C to a temperature of 350°C, with emissivity measurements being made during that process.
- ▶ After the pool had reached 350°C, it was then gradually cooled down to 200°C with further measurements of emissivity being made.
- ▶ It was then subjected to a further heating/cooling cycle in which the upper temperature was this time 450°C with emissivity measurements again being made throughout the cycle.
- ▶ A number of further shallow pool specimens were produced for similar tests. In all, 45 such tests were carried out.

Figure 8 shows that the emissivity values varied in a linear manner with temperature from 0.02 at 200°C to 0.03 at 450°C. Highly repeatable values of emissivity were obtained. Also shown on Figure 8 is a line which fitted the data obtained earlier by Tong in his overflowing sodium pool experiments (see Section 2). These covered a range of temperatures from 300°C to 600°C (the upper and lower lines shown indicate the uncertainty limits of his data). As can be seen from Figure 8, Lam's liquid sodium emissivity measurements line up extremely well with those of Tong and they extend the temperature range covered down to 200°C.

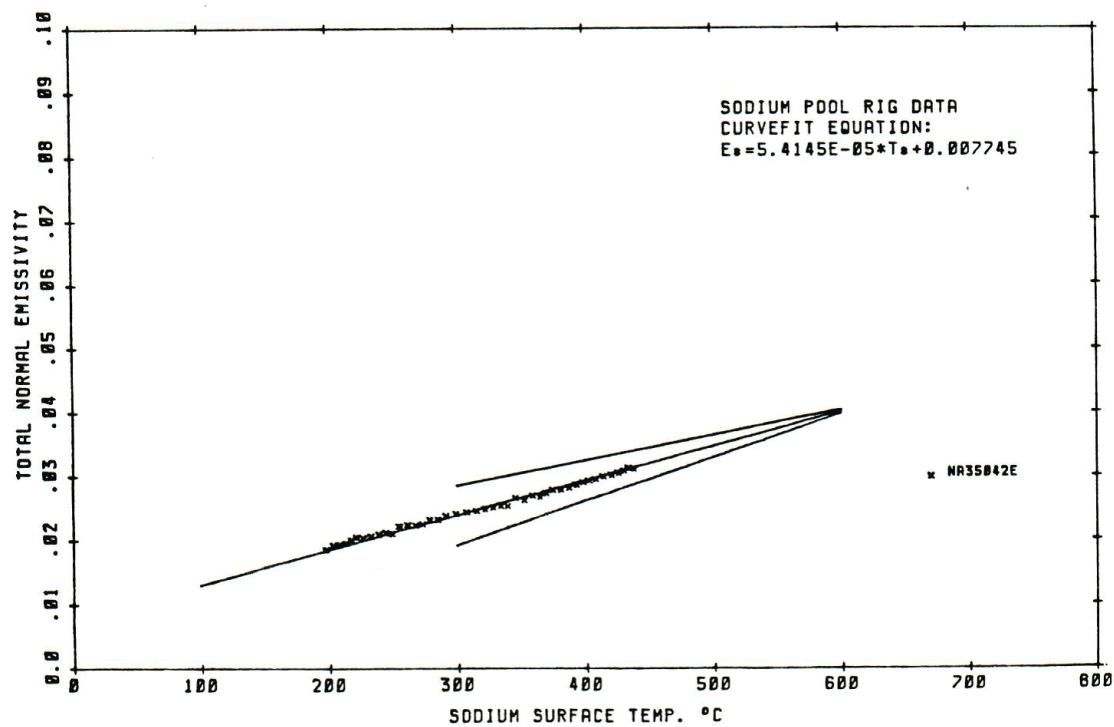


Figure 8: Emissivity of liquid sodium

5 Studies of Sodium Condensation

Lam [4] then went on to use the modified glove box test facility for the purpose of studying condensation of sodium on cooled downward facing stainless steel lids above a pool of liquid sodium in a vessel of internal diameter 50 mm. His studies revealed that there were basically two different modes of condensation, namely dropwise when the lid surface temperature was below 250°C and filmwise when it was above that temperature. This transition temperature was insensitive to both surface roughness and surface pre-oxidation. Thus, it was similar for machined stainless steel specimens and also 'as received, hot rolled' ones.

The emissivity of liquid sodium film covered specimens was measured by removing the lid, turning it over, mounting it on a heater block and then transferring it from the glove box to the thermal radiation measurement section. These emissivity values were found to be similar to, but slightly lower than, those measured by Lam in his earlier shallow pool experiments. The condensed sodium film was undoubtedly sufficiently thick (at least several hundred microns) that the steel surface underneath it was not involved in the thermal radiation emission process. Thus, the emissivity of the surface of the condensed film was that of pure distilled liquid sodium.

Measurements of the emissivity of the surface sodium film on the lid were made as a specimen from the condensation experiment was heated up slowly over a range of temperature from just over 250°C to 525°C. Figure 9 shows the results obtained from five separate tests on sodium-wetted specimens. It can be seen that the emissivity values are extremely consistent.

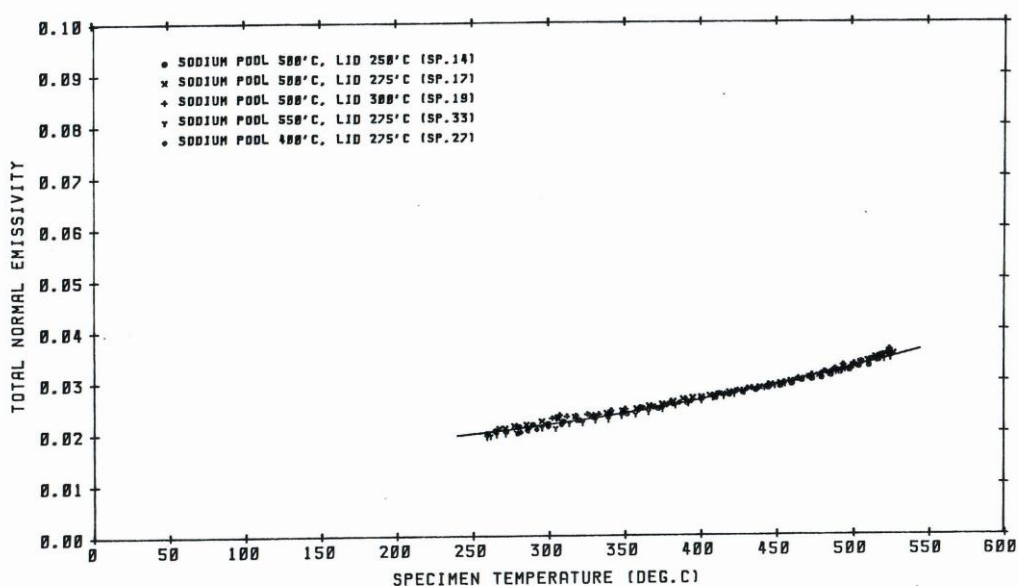


Figure 9: Liquid sodium emissivity data and curvefit for filmwise condensation

The data were fitted over the temperature range 250°C to 525°C using the least squares method by the second order polynomial equation:

$$\epsilon_s = 0.017 - 7.83 \times 10^{-6} T_s + 7.86 \times 10^{-8} T_s^2 \quad (2)$$

where T_s is in degrees Centigrade. All the measured data were found to lie within $\pm 5\%$ of the curve fit.

Figure 10 shows a comparison between the shallow pool results of Lam for reactor-grade sodium and those which he obtained for distilled liquid sodium in the condensation experiments.

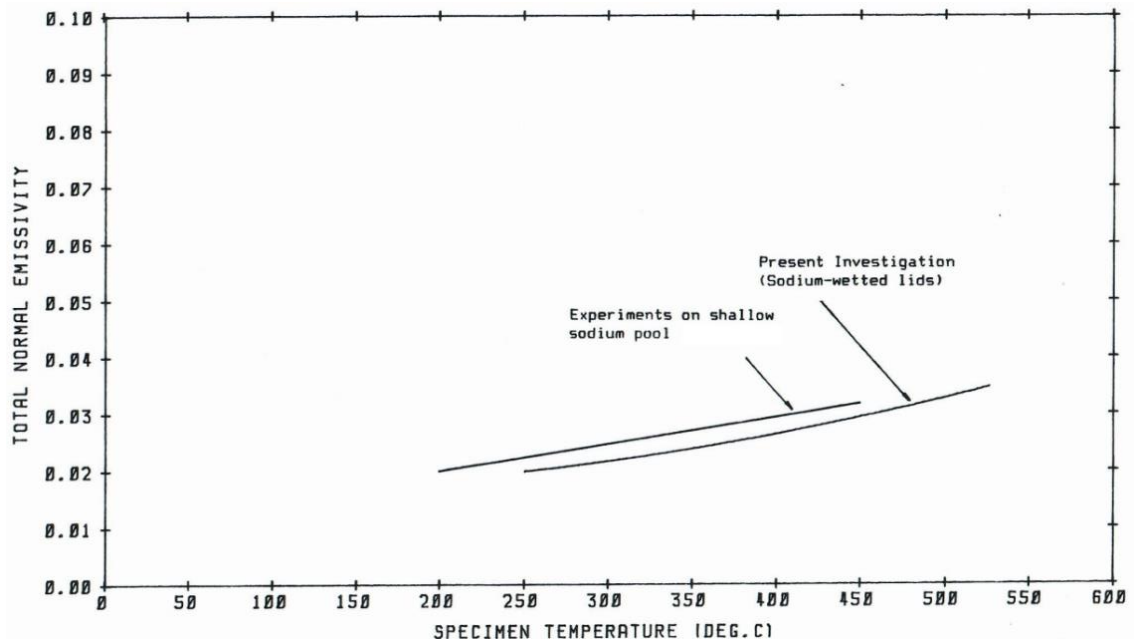


Figure 10: Comparison of two results for liquid sodium emissivity

The results from all the sodium emissivity measurements are presented together on Figure 11. The results from the experiments on the distilled sodium obtained in Lam's filmwise condensation experiments are very slightly lower than those for reactor grade sodium. The theoretical predictions from electromagnetic theory shown in Figure 11 are slightly higher than the experimental results.

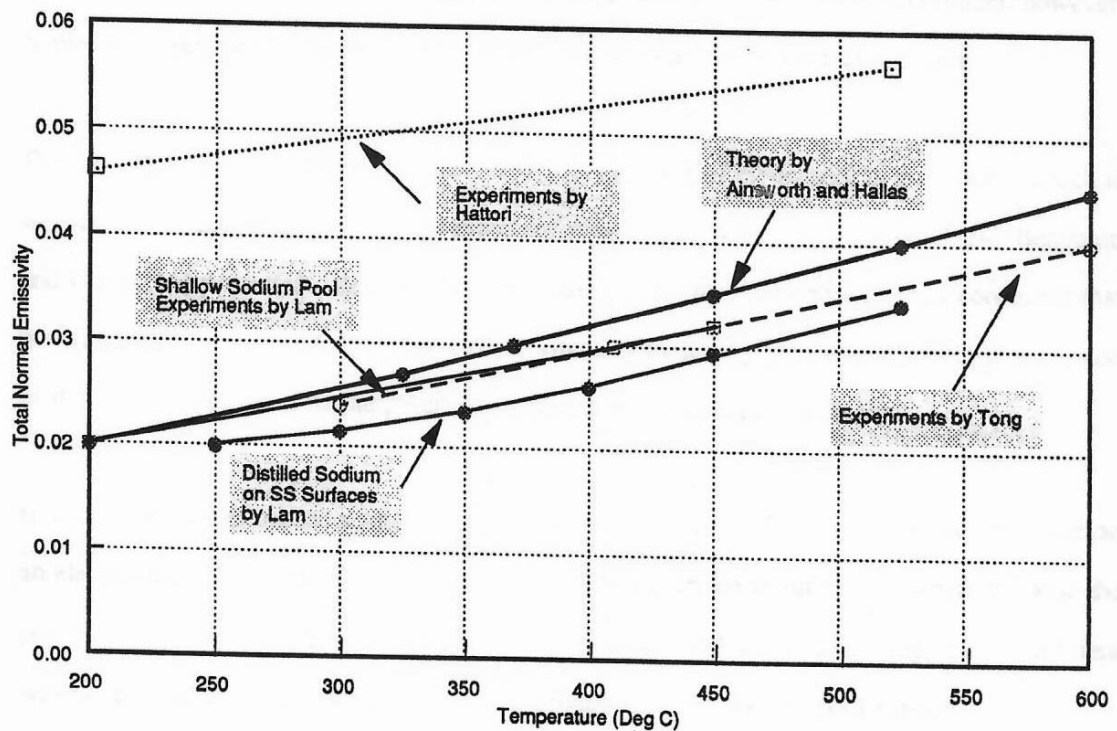


Figure 11: Comparison of four results for liquid sodium emissivity

6 Impact of Ripples on Emissivity

Experiments to measure the emissivity of the surface of an overflowing pool of liquid sodium and of a stationary shallow pool have been described in Section 2 and Section 4.2 respectively. However, in a sodium-cooled fast reactor, the free surface of the sodium pool is likely to be disturbed. Thus, it is of interest to examine the radiative properties of a rippled surface. This matter was addressed by a further PhD student, P. An [5].

A small square pool of sodium (40 mm by 40 mm by 10 mm deep) was mounted on an electromagnetically driven vibrator to generate ripples on the surface (Figure 12). This could be operated either in the glove box or in the thermal radiation measurement section (Figure 13). Ripples having a range of wavelengths and amplitudes were produced on the sodium pool surface.

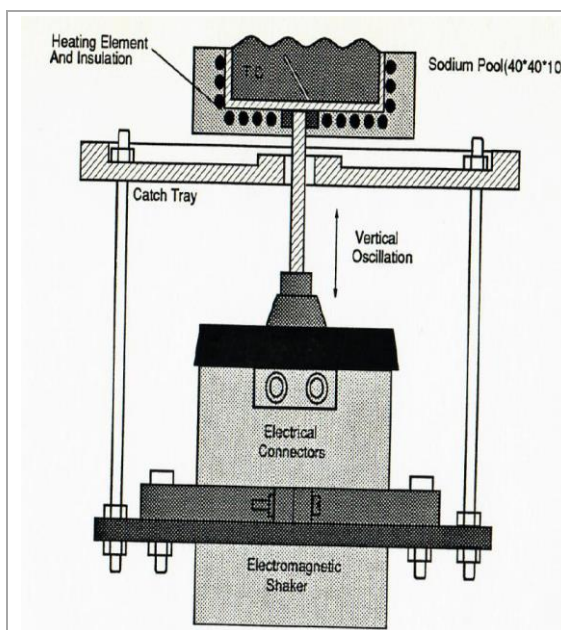


Figure 12: Liquid sodium ripple tank arrangement

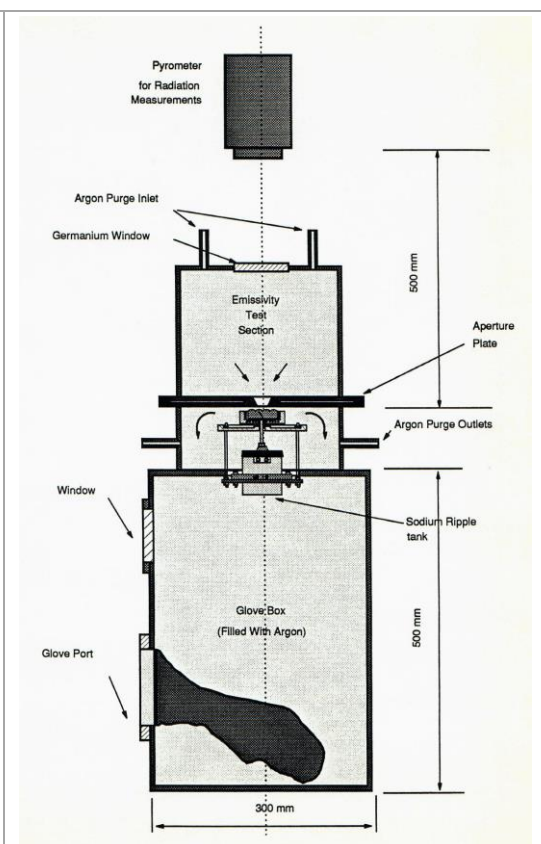


Figure 13: Sodium ripple tank in position in radiation measurement section

A lighting arrangement was installed in the glove box to enable the wavelength and amplitude of the ripples to be measured there. This was done for three temperature conditions (250°C, 275°C and 300°C) and at each temperature condition a range of oscillation frequencies and amplitudes were generated.

The assembly was then moved from the glove box into the radiation measurement section where the emittance of the surface was measured for each of the experimental conditions. In the course of making these measurements, the flow rate of the argon gas was adjusted to clear away any sodium aerosol cloud above the target area on the pool surface. This operation was aided by using a borescope to view the pool surface through the aperture plate. The overall

uncertainty in the measured emittance of a plane liquid sodium surface at a temperature of 250°C was about 15% (the liquid sodium emissivity was about 0.02).

The following observations were made in the course of these experiments (see An [5]):

- ▶ At certain amplitudes of vibration, ripples suddenly appeared on the surface. A subsequent increase in the amplitude of oscillation resulted in an increase in the amplitude of the ripples. The wavelength of the ripples decreased as the oscillation frequency was increased. Using a stroboscopic light, it was found that the ripples oscillated at a frequency half that of the liquid sodium pool container.
- ▶ Some enhancement of the emittance in the direction normal to the surface occurred when ripples were present. The biggest effect was found at low frequencies where the amplitude of the ripples was largest. For high frequencies, both the amplitude and the wavelength of the ripples were small and the effect on the total normal emittance was also small.

7 Impact of Dropwise Condensation on Emissivity

This section describes a programme of experimental work by Lam [4] to measure the emissivity of surfaces that promote dropwise condensation of liquid sodium on the lid of a small vessel. It was carried out using a modified version of the glove box test facility described in Section 4.2 (see Plate 2).

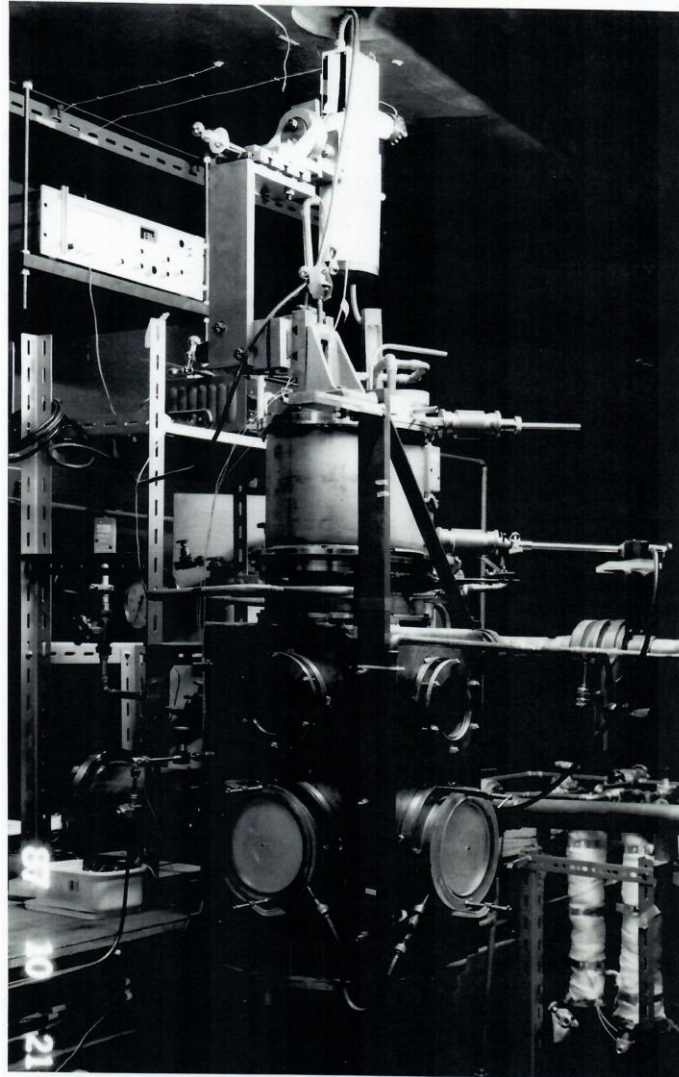


Plate 2: The modified glove box test facility

The sodium vessel, which had a height of 150 mm and an internal diameter of 50 mm, was operated inside the glove box. A schematic of the sodium vessel is shown in Figure 14. Sodium was melted into the bottom of the vessel to form a sodium pool about 10 mm in depth. Mineral insulated heating elements wound around the vessel enabled the side wall temperature to be controlled. Microtherm lagging was used to insulate the vessel.

Stainless steel sheathed and mineral insulated K-type thermocouples were located inside the vessel and on the side wall. The vessel was seated on top of a heater block which was used to control the temperature of the sodium pool. By controlling the power input to the vessel heater and the heater block, a variety of sodium pool, side wall and cover gas temperature conditions could be achieved.

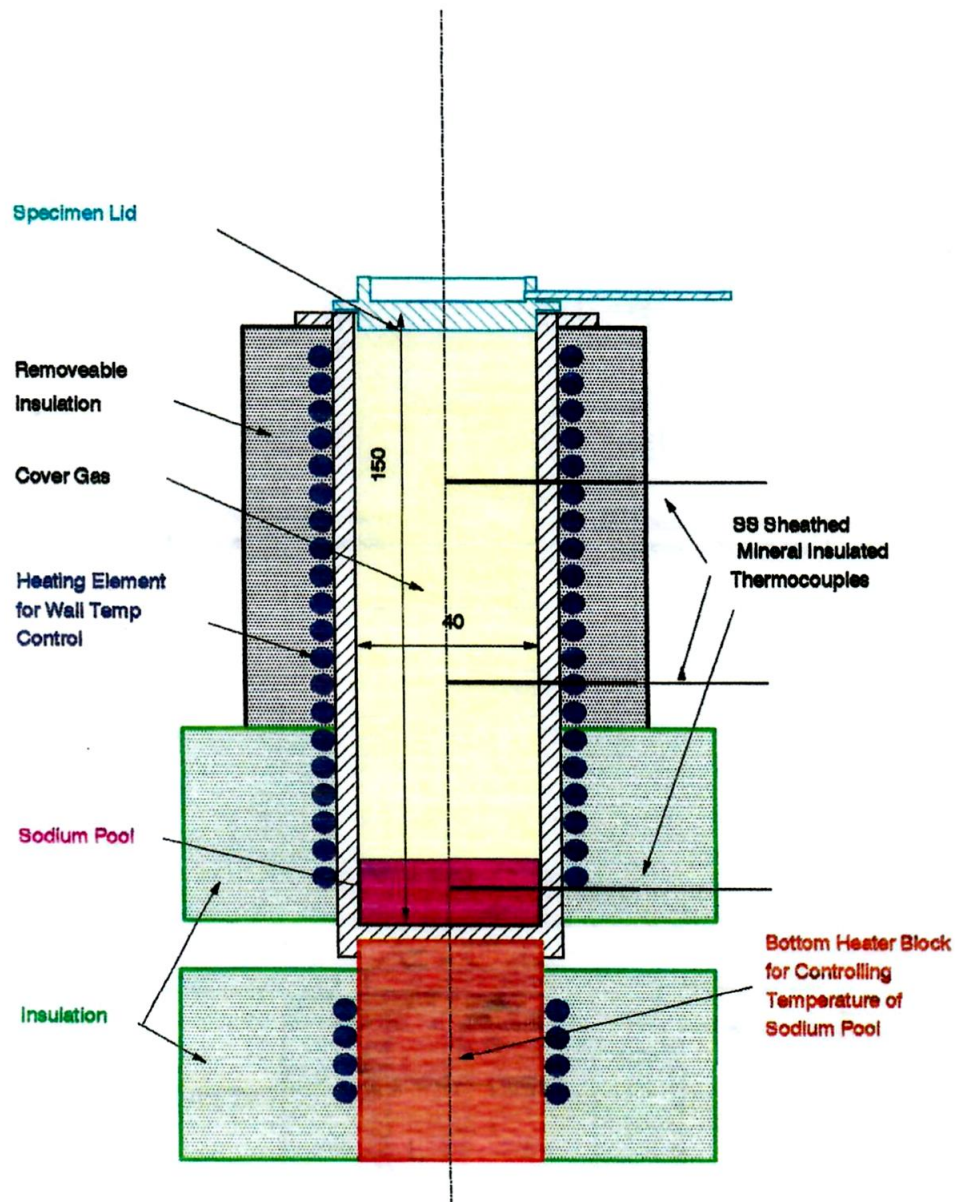


Figure 14: Sodium vessel arrangement

The sodium pool vessel with a lid in place is shown in Figure 14. A new specimen lid was used for each experiment. Dropwise condensation of sodium was promoted on the smooth underside of the lid for several different conditions of pool temperature and lid temperature and for various durations of exposure to sodium. The stainless steel vessel containing a pool of liquid sodium was situated inside the glove box in an argon atmosphere.

In each case, the lid was removed from the sodium pool vessel and then upturned and attached to the heater block after which it was transferred from the glove box to the radiation measurement test section (Figure 15).

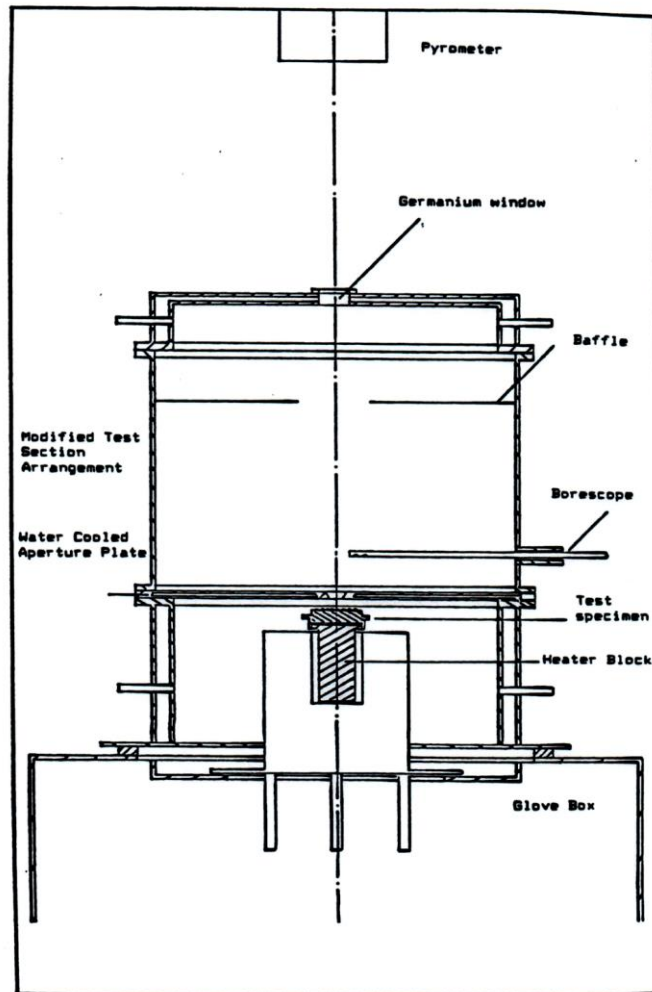


Figure 15: The arrangement for emissivity measurement

The lid was kept at the same temperature at which it had been maintained above the pool. The emissivity of the lid surface was then measured and the results are presented in Figure 16. The full line shows the variation of emissivity with temperature for filmwise condensation, which is described in Section 4.2 (see Figure 9).

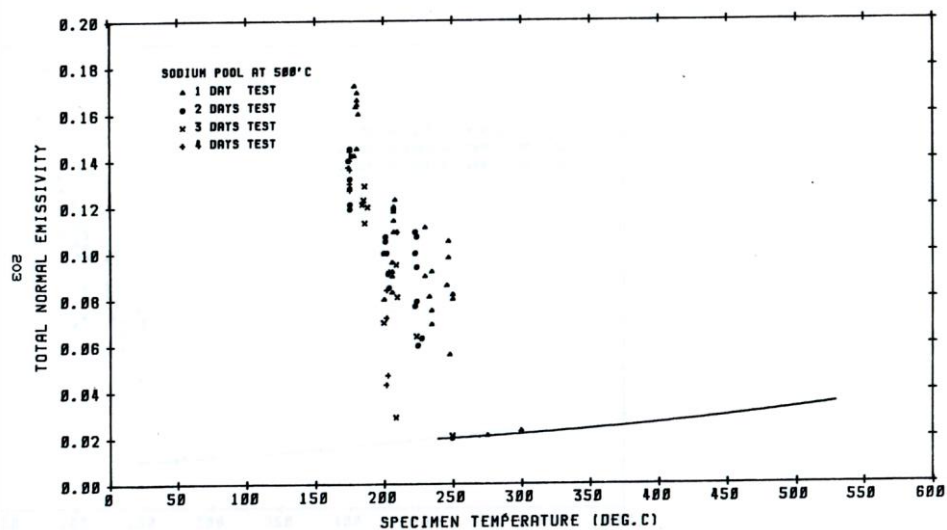


Figure 16: Emissivity of sodium droplet covered specimen surfaces – effect of exposure time for a fixed pool temperature

The specimen was moved laterally whilst being kept at a fixed temperature to enable the pyrometer to view different areas on the specimen. The mean emissivity value as a function of specimen temperature was worked out for each case and has been plotted on Figure 17.

The sodium condensation patterns were found to be similar to those for the smooth machined specimens, but there was a greater density of droplets on the 'as received' specimen than that of the machined finish.

The liquid sodium emissivity line for filmwise condensation (Figure 9 in Section 4.2) is included in Figure 17 for the temperature range 250°C to 525°C.

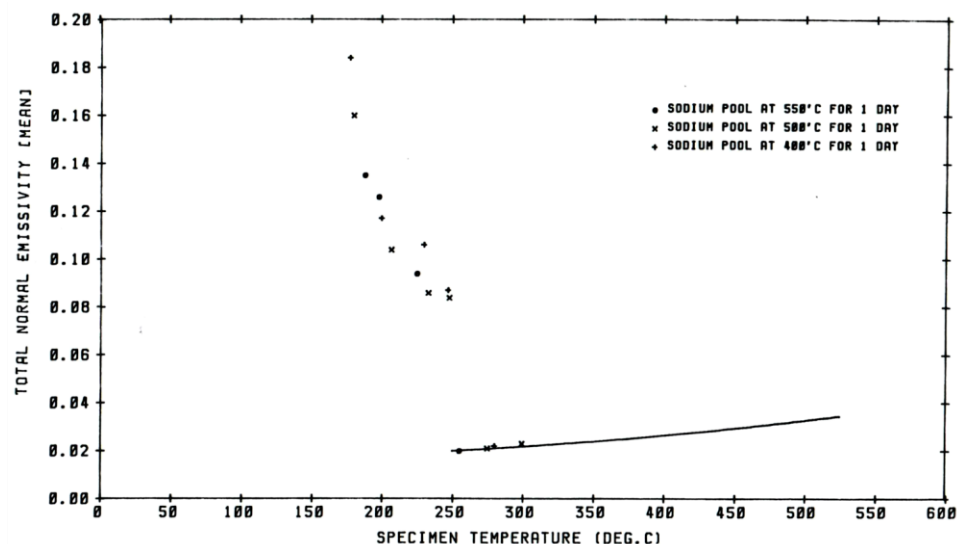


Figure 17: Mean emissivity of sodium droplet covered specimen surfaces – effect of pool temperature for fixed exposure time

The studies were extended to include dropwise condensation promoted on hot-rolled, de-scaled 'as received' stainless steel surfaces which had been treated above sodium for 2 days at a number of different specimen temperature values (175°C, 200°C, 225°C, 250°C, 275°C and 300°C) with a fixed sodium pool temperature (see Lam [4]).

8 Impact of Evaporation and Dryout on Emissivity

8.1 Single Dryout of a Sodium Film

This section describes measurements by Lam [4] of the emissivity of stainless steel specimens which were initially covered with a film of liquid sodium. These specimens were then subjected to a heating process leading to the complete evaporation of sodium from them. The initial condition was generated, by promoting filmwise condensation on specimens above a small pool of sodium. The specimens tested were either smooth machined stainless steel or hot rolled, de-scaled, 'as received', stainless steel (typical of materials used in sodium-cooled fast reactors).

After a specimen had been treated to produce the required initial condition of filmwise condensation on the surface, it was mounted on a heater block, transferred from the glove box up into the radiation measurement section of the glove box test facility (Section 4.2) and then heated to the point at which dryout of the surface occurred. Following this, the power setting was left unchanged and the specimen temperature settled at some higher value. The specimen was then allowed to cool down to a temperature of 175°C. Measurements of emissivity were made throughout the heating up and cooling down process. Photographs were taken using a borescope at certain stages as the temperature rose, to enable the drying out process to be studied.

Because the surfaces were covered by a film of liquid sodium as they were heated up from 250°C to 525°C, the emissivity values measured prior to onset of dryout were those of liquid sodium. The heating up of these sodium-wetted specimens was continued until the surface had completely dried out. A range of heating rates from 6.5°C/min to 10.5°C/min were applied.

Figure 18 and Figure 19 show the emissivity of film covered specimens of smooth machined steel during heating up to the dryout condition and subsequent cooling. In the experiments shown on Figure 18, the specimens had been at temperatures of 250°C, 275°C and 300°C whilst being treated above a sodium pool at 500°C. In the experiments shown on Figure 19, the specimens were at a temperature of 275°C above the sodium pool, but the pool temperature varied with values of 400°C, 500°C and 550°C.

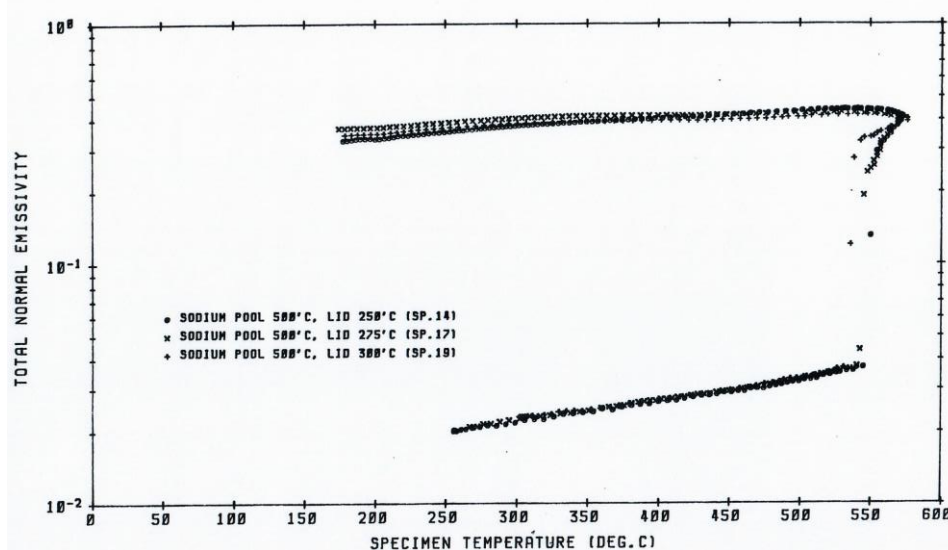


Figure 18: Emissivity of sodium film covered surfaces during and after dryout - Specimen temperatures of 250°C, 275°C and 300°C, Pool temperature of 500°C

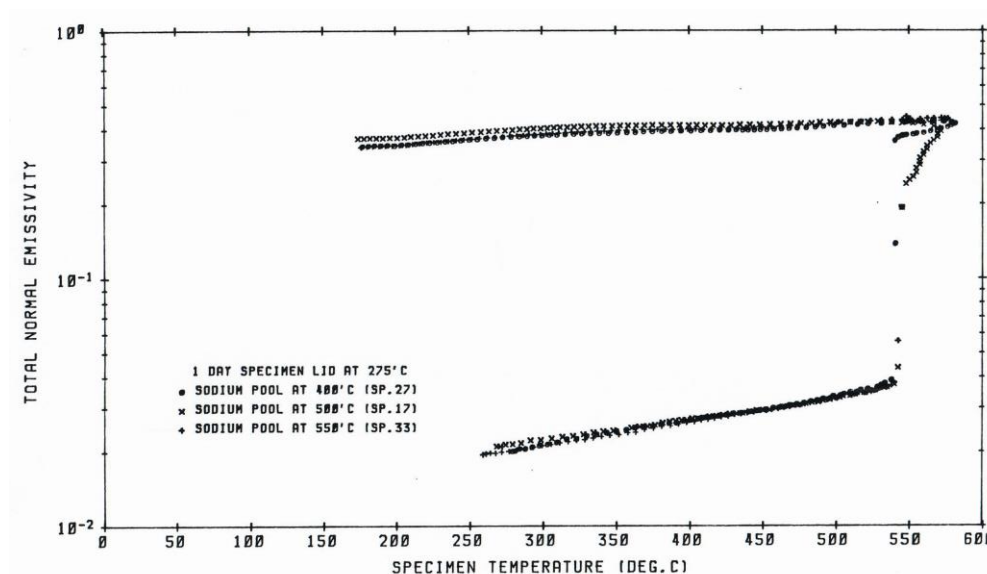


Figure 19: Emissivity of sodium film covered surfaces during and after dryout - Specimen temperature of 275°C, Pool temperatures of 400°C, 500°C and 550°C

It can be seen that the emissivity of the specimens after dryout was very repeatable and in the range from 0.45 at 575°C to 0.35 at 175°C.

The measured emissivity values after complete dryout were much higher than those of clean machined steel which would have been in the range from 0.15 to 0.18 over the range of temperature covered. The steel surfaces were stained after the sodium had been evaporated from them. The specimen temperature at dryout was found to be between 535°C and 550°C.

As mentioned earlier, similar experiments were also carried out using hot-rolled, de-scaled, 'as received' stainless steel specimens and these produced similar results.

8.2 Repeated Dryout of Sodium Filmwise Condensation

The structural surfaces in the cover gas region of a sodium-cooled fast reactor are in contact with sodium-laden cover gas. Accumulation of liquid sodium on such surfaces could lead to chemical reactions between the steel surfaces and sodium which will change the surface conditions and influence their radiative properties. Information about the likely effects on the radiative properties of such surfaces is needed.

Experiments were also carried out by Lam [4] using the improved glove box test facility to study the effect of repeated filmwise liquid sodium accumulation and subsequent dryout on the radiative emittance from machined and 'as received' stainless steel specimens. These specimens were machined in the form of lids fitted on the top of the small sodium pool described earlier in Section 8.1. Three K-type thermocouples were embedded in the specimen lid near to the test surface.

A specimen lid was placed on top of the sodium vessel and filmwise condensation/deposition was promoted on it with the sodium pool at a temperature of 550°C and the specimen at a temperature of 290°C.

After a period of time, the specimen became covered by a film of liquid sodium. It was then removed from the vessel, upturned, mounted on the heater block, photographed and transferred to the radiation measurement section. During the emissivity measurements which followed, the

specimen was heated up at a rate of about 3-4°C/min, with the emittance being measured at regular intervals until the emissivity suddenly rose to a high value indicating that the film of liquid sodium had evaporated from the surface. The specimen was then allowed to cool down to 290°C with the emittance measurements continuing.

Next, the specimen was again placed in the sodium vessel in the glove box to promote further filmwise deposition of sodium at the same temperature conditions. It was then transferred back to the radiation measurement section and the heating up to dryout followed by cooling was repeated again with care being taken to locate the specimen in the same position. These procedures were repeated again and again until the post-dryout total normal emittance of the surface had reached a steady value.

The emittance of the smooth machined and 'as received' specimens undergoing repeated cycles of filmwise liquid sodium deposition followed by dryout is shown on Figure 20(a) and Figure 20(b), respectively. In the first stage of each radiation measurement sequence, the emittance of the surface was found to be that of a plane clean liquid sodium surface (which is between 0.02 to 0.035 over a temperature range from about 300°C to 500°C). When the specimen reached the temperature at which the liquid sodium film dried out, the emittance then suddenly increased dramatically. The post-dryout emittance temperature remained high as the specimen cooled down. This temperature increased gradually after each cycle, and then on cooling down eventually levelled out at about 0.9 after 7-8 cycles. The appearance of the surfaces became progressively darker and darker.

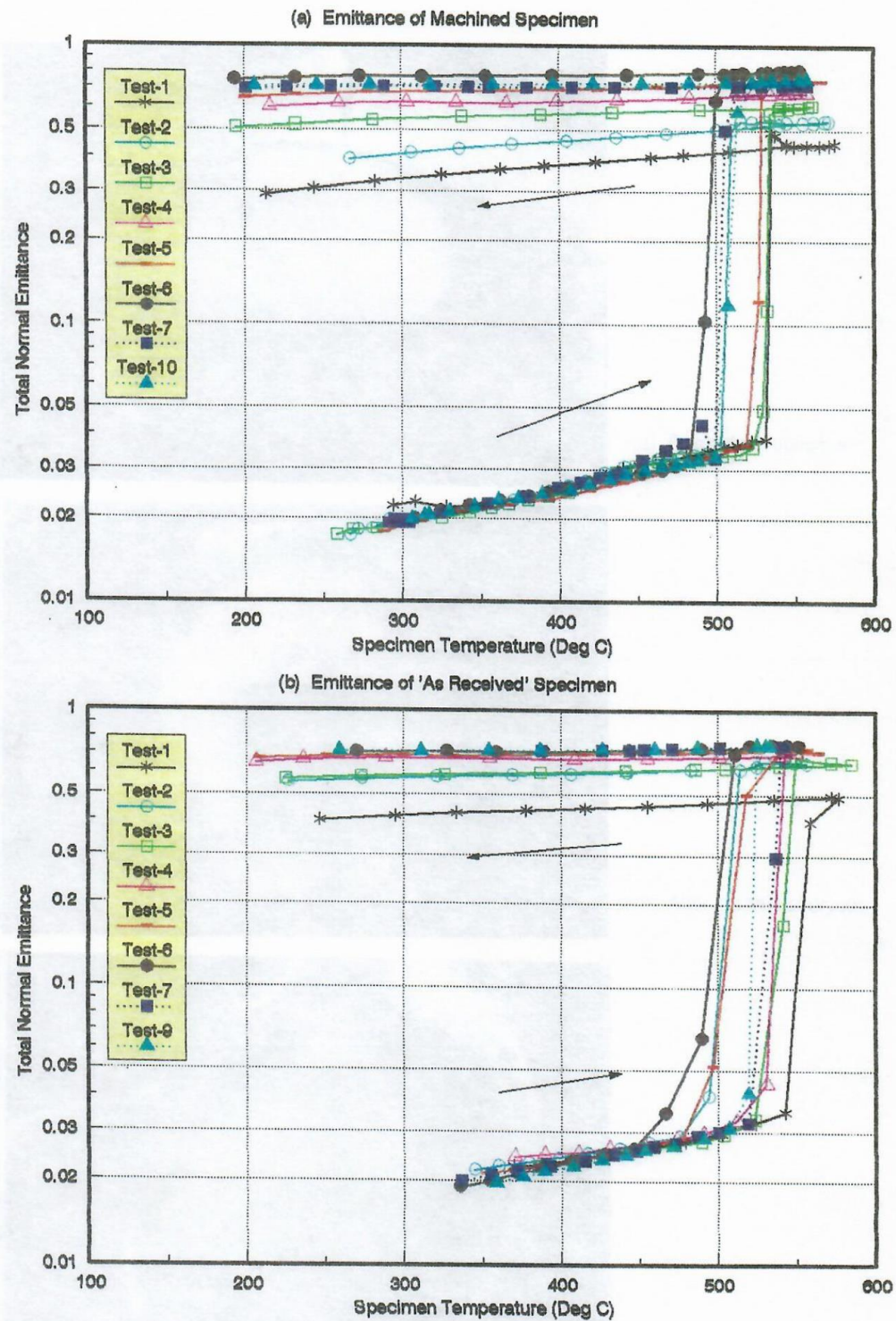


Figure 20: Total normal emittance of 'as received' and machined specimens undergoing repeated filmwise deposition and subsequent dryout

It is apparent that chemical reactions occurred during the period of promoting liquid sodium deposition on the specimen surface and also in the course of the emittance measurement in which the specimen was heated up to the point of dryout.

9 The MUSAC Research Project

The Manchester University Sodium Aerosol Characteristics (MUSAC) research project was initiated in 1987. It was carried out with the aim of obtaining information about the sodium aerosol laden cover gas region in fast reactors and also the rate of heat transfer through it from the pool surface to the reactor roof.

9.1 Preliminary Studies of the Sodium Aerosol Cloud

Preliminary studies were undertaken by Burns [6] and Anderson [7] during 1987 and 1988. Two different particle sizing instruments were tried out. The first one (the Malvern Instrument) involved using laser light scattering and the second one (the Jet Impactor) involved impaction and collection of sodium aerosols. Some useful preliminary data on sodium aerosol concentration and size distribution were obtained using both those instruments with a small scale sodium pool test facility prior to a more detailed study. Figure 21 and Figure 22 show examples of some preliminary results using the Malvern Instrument.

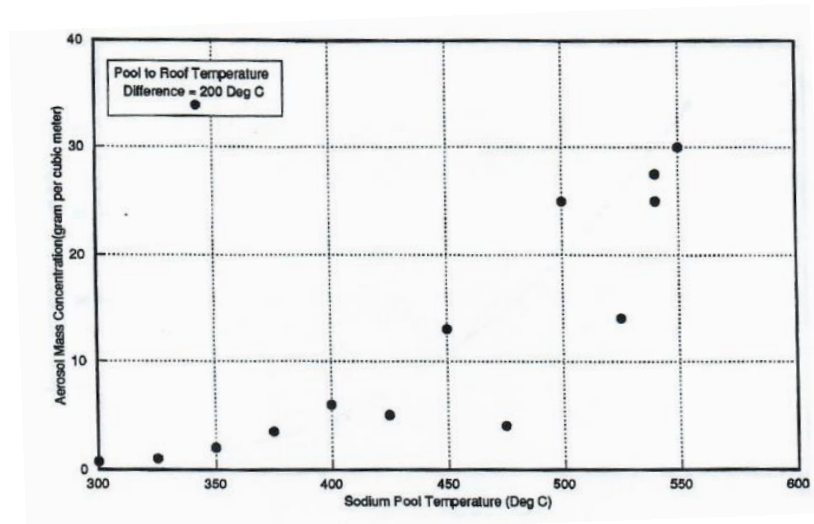


Figure 21: Aerosol concentration as a function of pool temperature

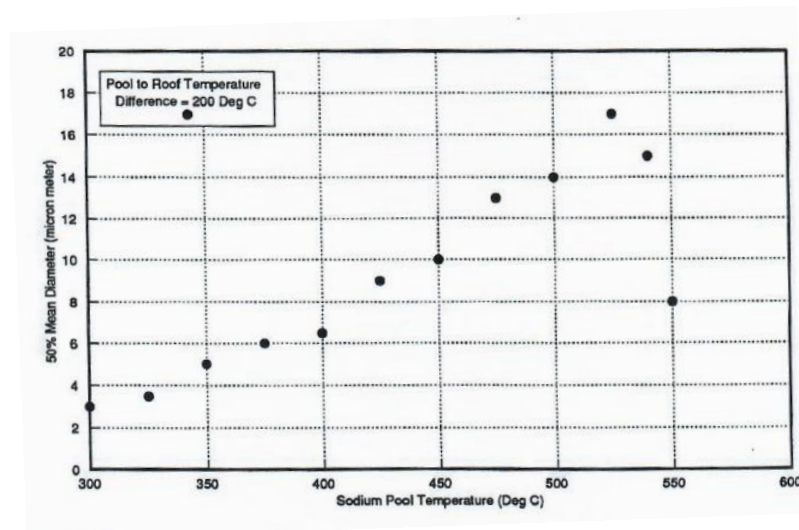


Figure 22: Mean diameter of the sodium aerosol as a function of pool temperature

9.2 Description of a Large Scale Sodium Pool Test Facility (MUSAC)

The test facility had a sodium pool test section of 780 mm diameter. It was designed and commissioned in 1988 and 1989 by Anderson [7] for an experimental study aimed at providing detailed information concerning:

- ▶ Aerosol size distribution and concentration in the cover gas region above a sodium pool;
- ▶ Cover gas temperature distribution;
- ▶ Rate of deposition of sodium on the side wall of the test section; and
- ▶ Rate of heat transfer to the roof of the test section.

A full description of the test facility including the features needed for all of these measurements can be found in An [5]. A schematic diagram of the test facility is shown below on Figure 23.

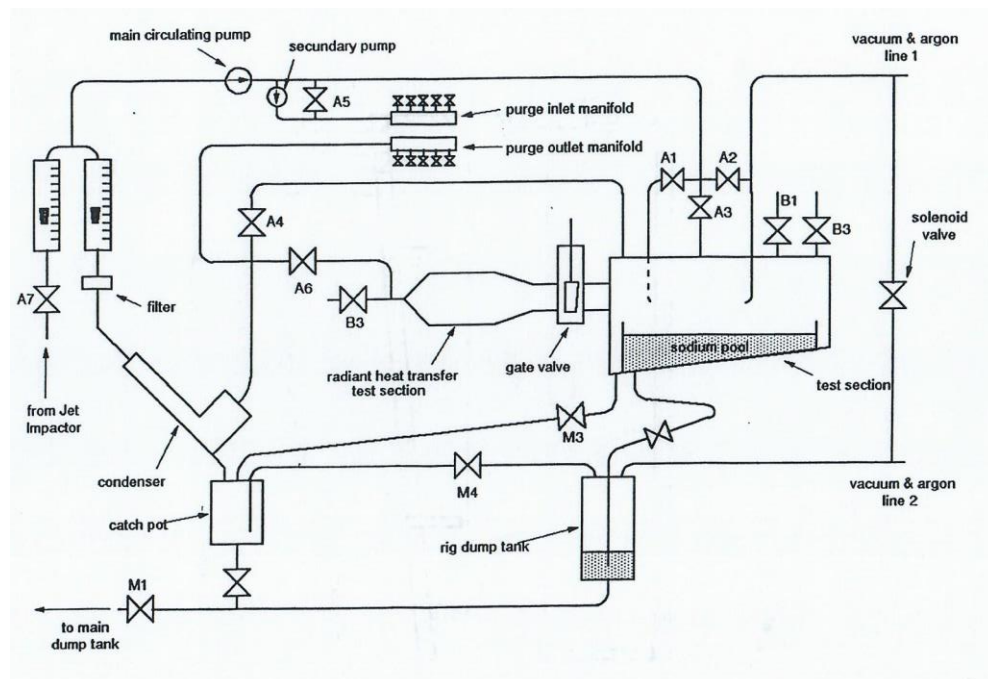


Figure 23: Schematic diagram of the test facility

The test facility was a cylindrical vessel of diameter 800 mm and height 320 mm at the shallow end and 390 mm at the deep end with a 780 mm diameter sodium pool. The base of the test section was inclined to facilitate draining the sodium back into the dump tank which was directly below the test section. The test facility had its own argon/vacuum system lines. The pressure in the dump tank could be adjusted independently of that in the sodium pool test section. By pressurizing it, sodium could be transferred to the test section via the pipe shown.

An external argon circuit was provided to enable samples of cover gas to be drawn from the test section and passed through a Jet Impactor for the purpose of measuring the concentration and the size distribution of the aerosols. It was possible to draw argon continuously from the cover gas space, strip it of any sodium vapour and aerosol, and re-inject it back into the test section. The argon circuit comprised of a condenser, a filter, a primary circulating pump, a secondary pump for the purge system and three flowmeters. These were used to independently measure the argon flow rates through the Jet Impactor, the purge lines and the cover gas space.

Any sodium that collected in the condenser was allowed to drain into an additional vessel, referred to as the catch pot. This could also receive sodium that condensed on, and

subsequently drained from, the side wall of the test section. Sodium could be transferred later from the catch pot to the dump tank. The side wall of the test section needed to be thermally independent of the base and the roof to enable the wall to be maintained at a uniform temperature similar to that of the cover gas. The roof of the test section was maintained at a fixed temperature of 120°C by blowing air from an array of fans mounted approximately 1 m above the roof (see Figure 24). The cooling fans were then switched off and a layer of insulating material was placed on the roof. The roof temperature then increased in a transient manner. The rate of temperature rise could be used to determine, the total rate of heat transfer to the roof from within the test section.

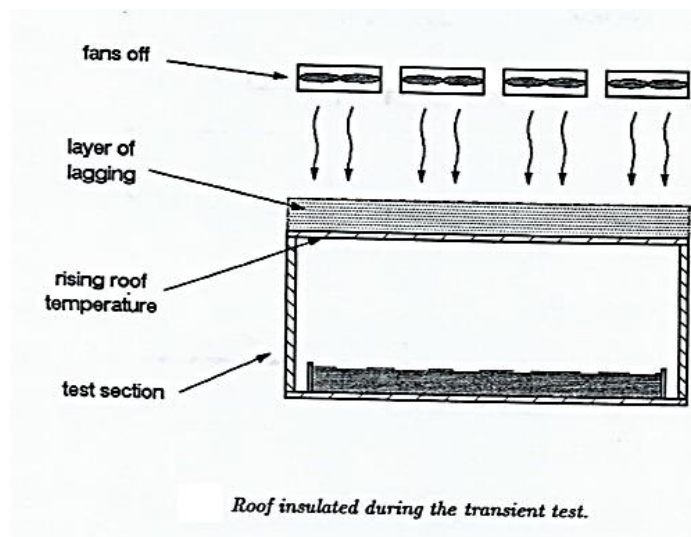


Figure 24: Initial arrangement for determining the rate of heat transfer to the roof

Later, the rate of heat flow was also measured using seven commercially available heat flux meters. When operating with the heat flux meters on the roof, it was found that there was a significant systematic variation between the readings from the various devices. The arrangement was improved by putting a 9 mm thick uniform layer of carbon steel shot (approximately 0.3 mm in diameter) on top of the roof. This was sandwiched between the stainless steel roof and the mild steel top plate (see Figure 25). This prevented the heat flux sensors from being in direct contact with the cooling air.

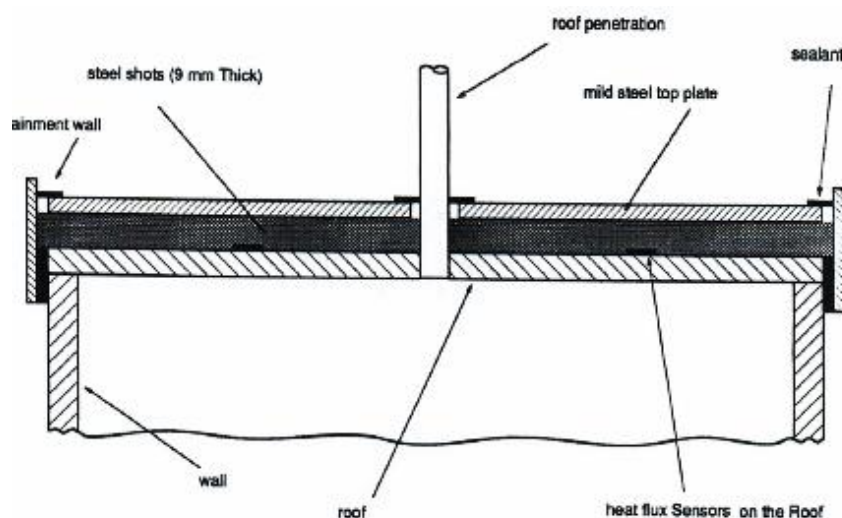


Figure 25: Roof showing the heat flux sensors, the iron shot layer and the top plate

9.3 Commissioning Tests

The test facility was first charged with sodium from the main laboratory dump tank and central supply/clean-up system in June 1989. Plate 3 shows a photograph of the test facility during commissioning.

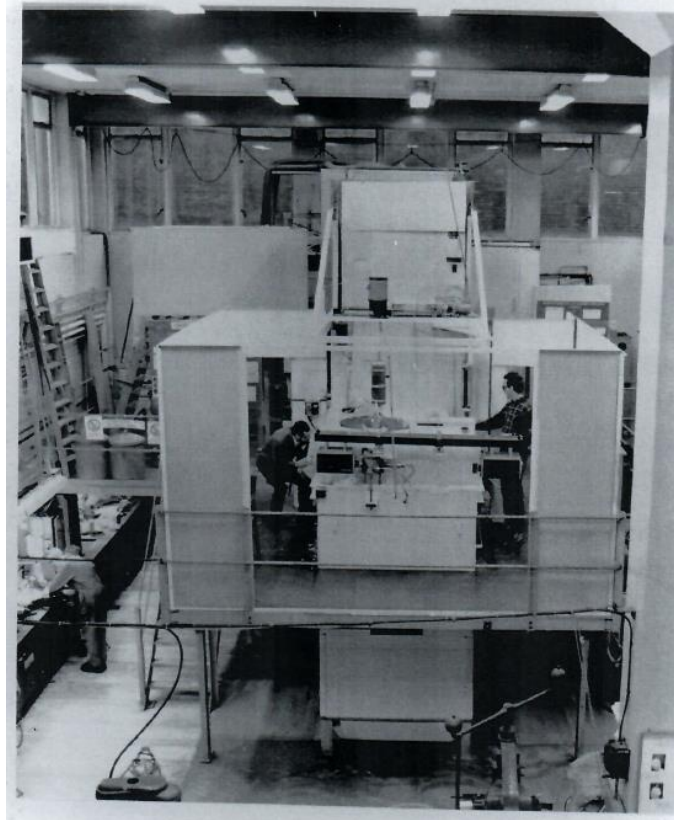


Plate 3: Photograph of the sodium pool test facility during the initial stage of operation

Commissioning tests were performed in 1989 by Anderson. Each test involved heating up the test section to some pre-defined temperature condition. By carrying out a number of tests under various conditions, it was possible to establish the effect of each of the various parameters involved (for example the pool temperature) on the quantities being measured.

9.4 Initial Programme of Experimental Work on the MUSAC Test Facility

The initial programme of experiments using the test facility was carried out by Anderson and commenced in January 1990. It concentrated mainly on making detailed measurements of the characteristics of the sodium aerosol cloud in the cover gas above the sodium pool. Initially four series of experiments were performed and these will be referred to as Series A, B, C and D. Each series was carried out to investigate the effect that varying a particular parameter had on the quantities being measured:

- ▶ **Series A:** This was carried out to investigate the effects of varying the sodium pool temperature. The roof of the test section was maintained at 120°C and a number of experiments were performed in which the pool temperature was progressively increased from 350°C to 550°C in steps of 50°C. The temperature of the side wall was in all cases maintained close to the cover gas temperature (see An [5]).
- ▶ **Series B:** Eight experiments were carried out in which the pool and the roof temperatures were maintained at 550°C and 120°C respectively. The side wall temperature was again

adjusted so that it was close to that of the cover gas. The aim was to decide whether the conditions of the wall and roof surfaces might possibly change gradually in time due to sodium deposition.

- ▶ **Series C:** This series of experiments was carried out to investigate whether sampling at different positions in the cover gas space would yield different aerosol characteristics as measured using the Jet Impactor. Six different sampling positions were tried, as illustrated in Figure 26. The temperature conditions were identical to those of Series B (that is 550°C pool temperature and 120°C roof temperature).
- ▶ **Series D:** This series of experiments was carried out to investigate the effects of varying the side wall temperature. Whereas in all the previous tests the wall temperature had been maintained close to that of the cover gas throughout the experiment, in this series the wall temperature was varied from about 60°C below the cover gas temperature to about 60°C above it.

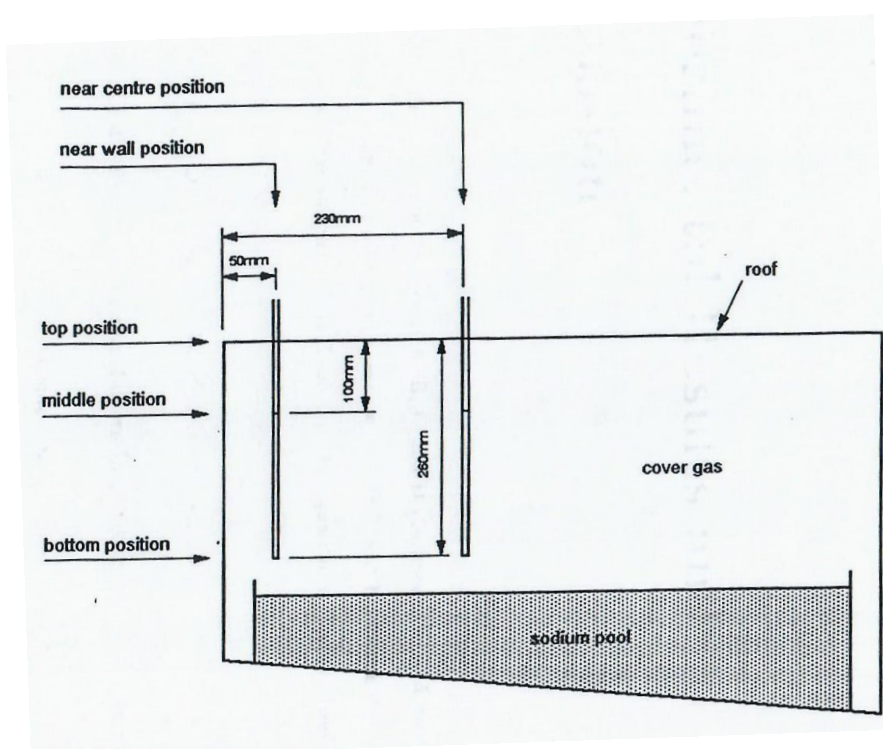


Figure 26: Different sampling positions for the Jet Impactor

9.5 Results from the Initial Programme of Experimental Work

9.5.1 Cover gas aerosol characteristics

(a) Aerosol concentration

The mass concentrations of sodium aerosol measured during the Series A tests are presented on Figure 27. The graph shows the results from both the Malvern Instrument measurements and the Jet Impactor measurements, plotted against the sodium pool temperature. It can be seen that the Jet Impactor results were always slightly lower than the Malvern results. Some discrepancy was to be expected since a small proportion of the sodium aerosol would be deposited along the length of pipe that takes the sample from the cover gas space to the Jet Impactor (approximately 300 mm in length). Traces of sodium were visible in the pipe. Thus, the results obtained using the Jet Impactor were likely to be slightly below the actual values.

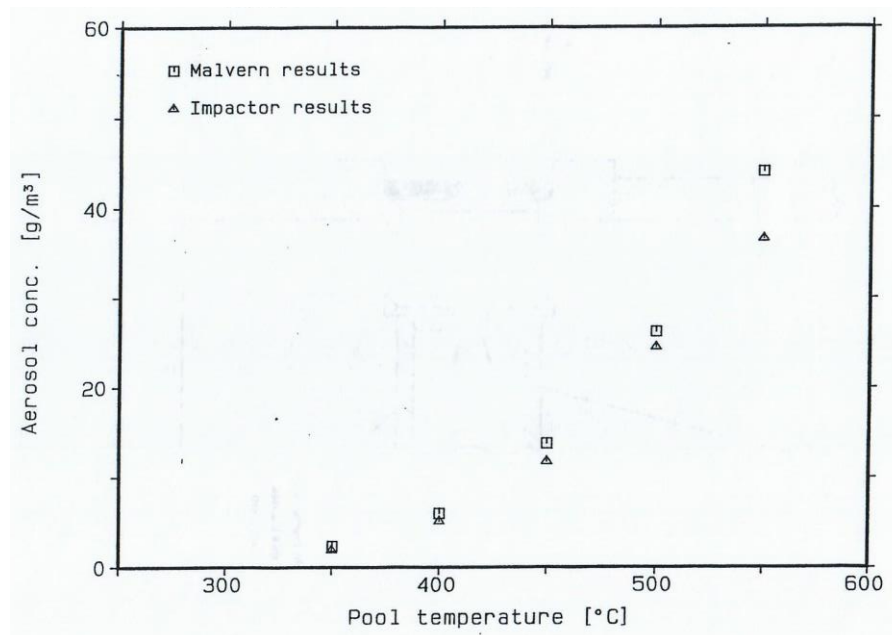


Figure 27: Aerosol concentration against sodium pool temperature

In Figure 28, the aerosol concentration is plotted on a log-log basis against an evaporation rate parameter. The parameter chosen to be representative of the evaporation rate was $Ra^{1/3} \times c(T_p)$, where Ra is the Rayleigh number based on the sodium pool diameter, T_p is the temperature of sodium pool surface and $c(T_p)$ is the mass fraction of saturated sodium vapour in the argon at the temperature T_p . The linear behaviour indicates that a simple power law relationship between the measured aerosol concentration and this parameter exists. The approach was arrived at by invoking an analogy between heat and mass transfer.

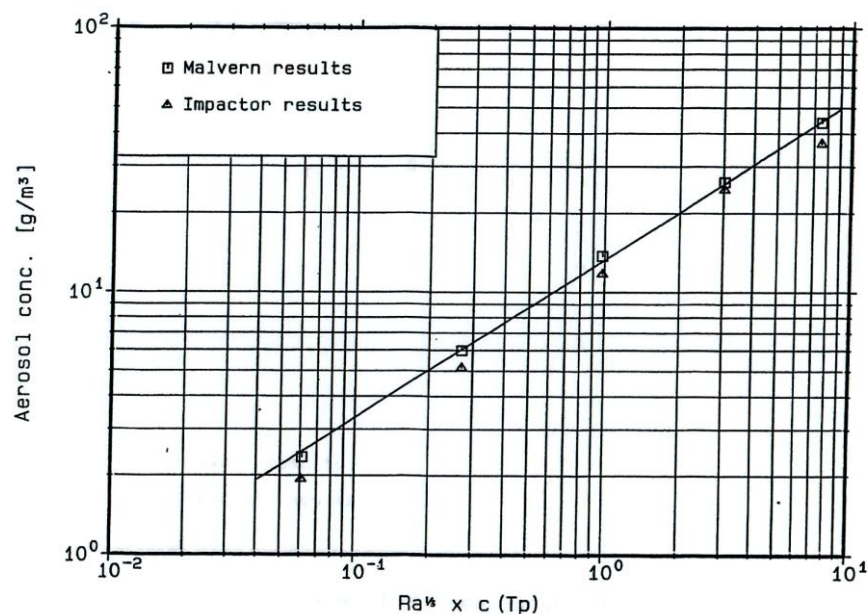


Figure 28: Aerosol concentration against evaporation parameter

In Series C, the Impactor sampling position was varied to determine whether any spatial variation in the aerosol concentration existed in the cover gas region. The results are plotted in Figure 29, where different markers have been used to identify the various sampling positions.

There does not appear to be any systematic variation in the aerosol concentration with either vertical position or distance from the side wall.

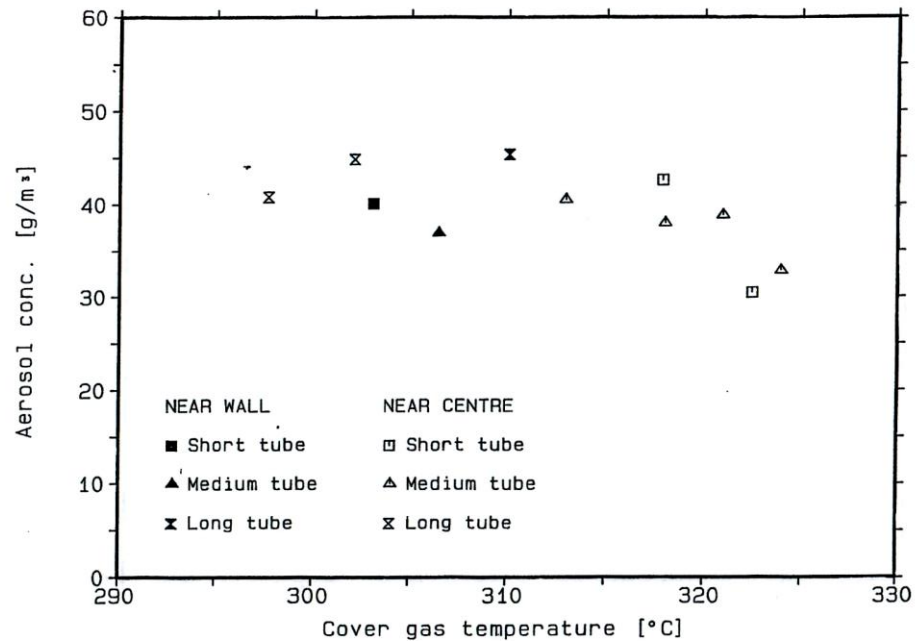


Figure 29: Aerosol concentration at different Impactor sampling positions

(b) Size distribution and mean diameter of the aerosols

Figure 30 shows the aerosol mean diameters plotted against sodium pool temperature for the Series A tests. The diameters chosen for the plot are the 50% diameter by volume (particles with diameters smaller than this constitute 50% of the total volume of aerosol). Although there is very good agreement between the Jet Impactor and the Malvern results at low pool temperature, some discrepancy is evident at higher temperatures.

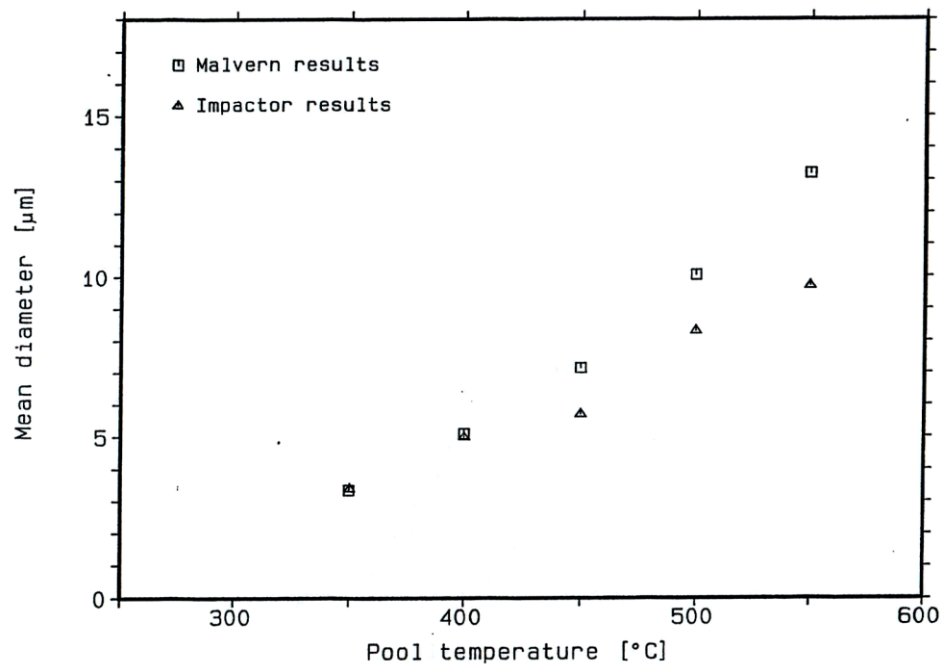


Figure 30: Aerosol mean diameter against sodium pool temperature

The size distributions were found to be well fitted by the Weibull distribution function

$$v(d) = \frac{\beta d^{(\beta-1)}}{\eta^\beta} \exp\left\{-\left(\frac{d}{\eta}\right)^\beta\right\} \text{ with the shape factor, } \beta, \text{ between 3 and 3.5.}$$

Figure 31 shows the aerosol size distribution information:

- ▶ The histogram shows the results obtained using the Malvern Instrument interpreted using a model independent technique. In this technique, the size distribution is divided into 24 discrete bands.
- ▶ The solid line is a model dependent solution in which a Weibull distribution function was fitted to the Malvern data.
- ▶ The distribution marked (+) represents a Weibull distribution function fitted to the Jet Impactor data.

As can be seen from Figure 31, there was good agreement between the Malvern and the Jet Impactor results.

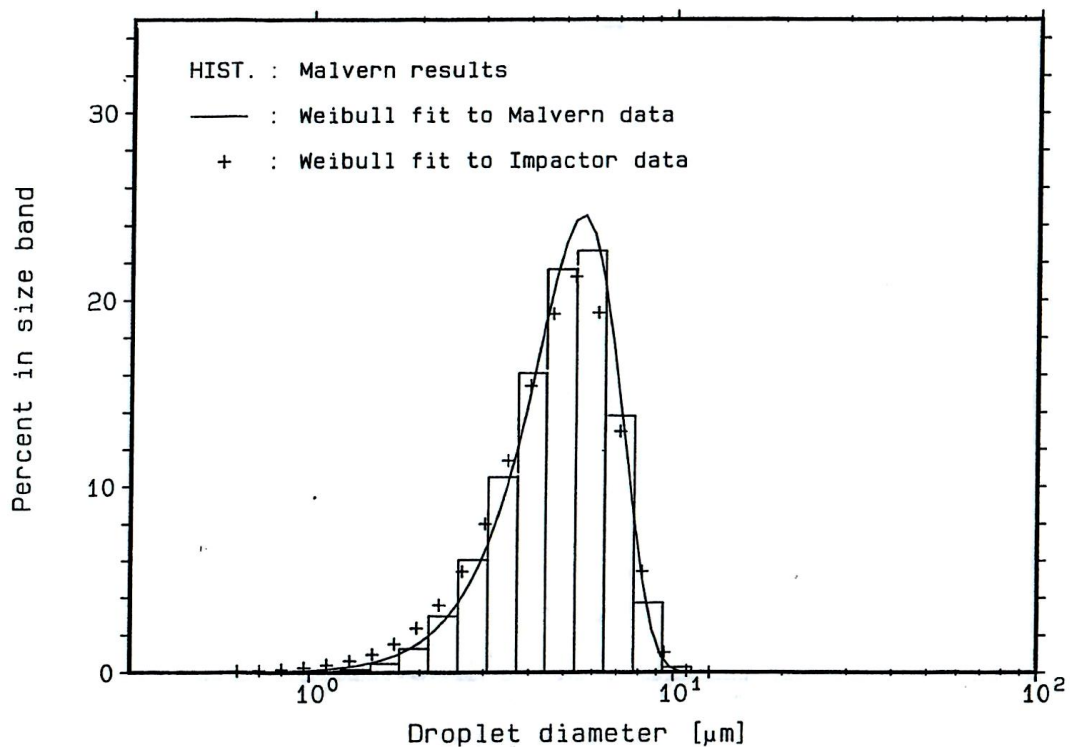


Figure 31: Size distribution of sodium aerosol, test No. 23

Figure 32 shows the aerosol mean diameters plotted against cover gas temperatures. The results shown in the figure are those obtained using the Malvern Instrument.

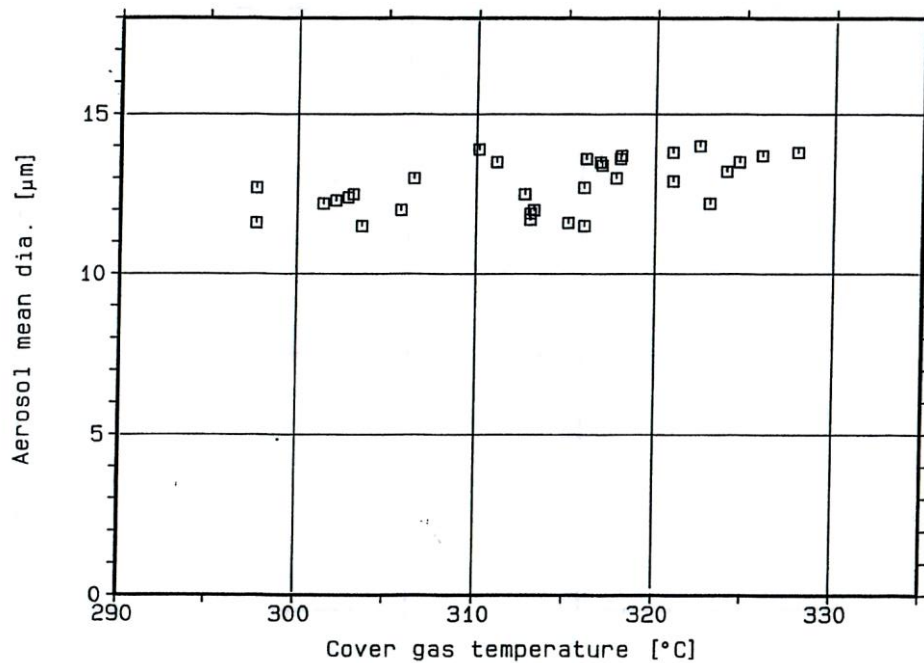


Figure 32: Aerosol mean diameter against cover gas temperature for Series B, C and D

As mentioned earlier, the aerosol volume distributions were well fitted by a Weibull distribution function. The mean diameters (η) and shape factors (β) are shown on Figure 33 and Figure 34 for the Series A and B results respectively.

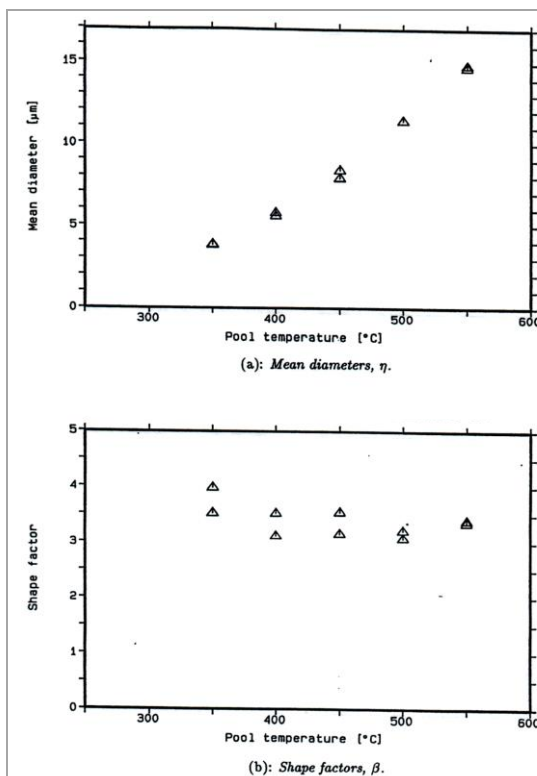


Figure 33: Parameters of the Weibull size distribution functions for the Series A results

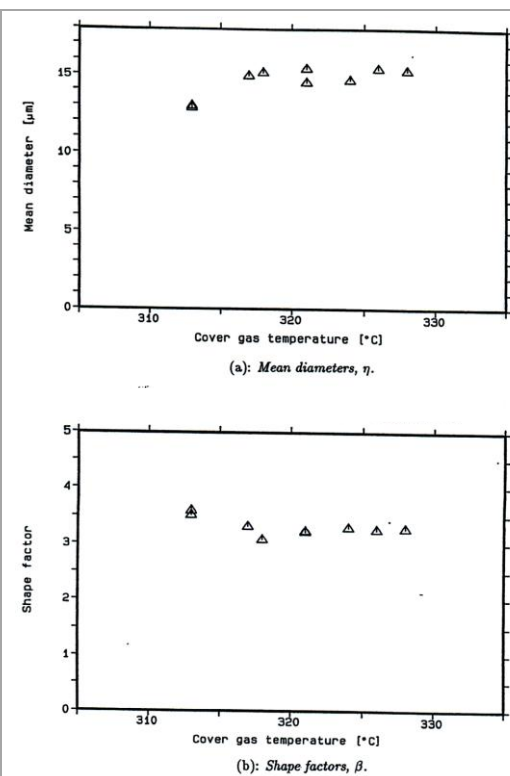


Figure 34: Parameters of the Weibull size distribution functions for the Series B results

9.5.2 Cover gas temperature profiles

As described in An [5], the temperature of the cover gas was monitored by two combs of thermocouples: a fixed comb and a traversing comb. The temperature profiles were similar in all of the tests carried out. Typical temperature profiles are shown in Figure 35(a) and (b).

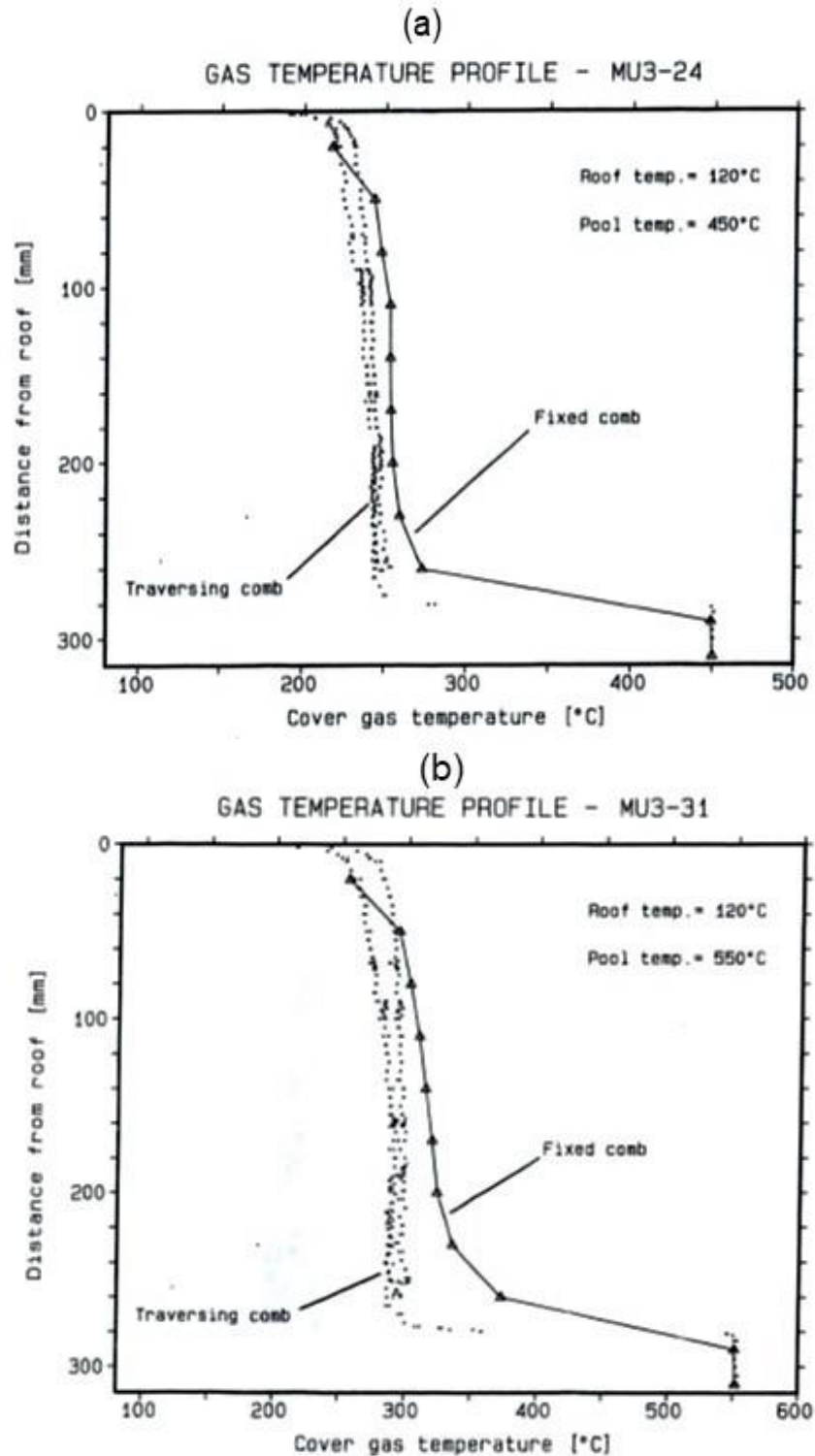


Figure 35: Cover gas temperature profiles (a) for test No. 24 and (b) for test No. 31

The results obtained from the fixed comb thermocouples have been emphasised by joining the individual data points by straight lines. The temperatures measured by thermocouples on the traversing comb are represented by single dots and were obtained by gradually moving the comb downwards over a period of approximately 20 minutes.

The main feature of the temperature profiles is that most of the temperature change occurs in thin layers near the pool surface and near the roof. This is consistent with the fact that the Rayleigh number for the convective process in the cover gas space is fairly high (between 10^7 and 10^8) indicating that the motion is likely to be turbulent. The bulk of the cover gas is, therefore, likely to be well mixed and this has been confirmed by observations of the cover gas through the sapphire window (see An [5]). The level of turbulence observed explains why no systematic variation of aerosol concentration were detected by sampling at different positions in the cover gas space with the Jet Impactor.

A number of features of the temperature profiles warrant some explanation. The thermocouple arrangement was not ideal for measuring the temperature distribution accurately within the thermal boundary layers, particularly near the liquid sodium pool surface. The thermocouples were relatively thick (1 mm in diameter) and not shielded from thermal radiation. The temperatures measured by the thermocouples on the traversing comb were higher than those measured by thermocouples on the fixed comb in most of the tests. A possible explanation of this is that the cover gas was circulating in the manner illustrated on Figure 36.

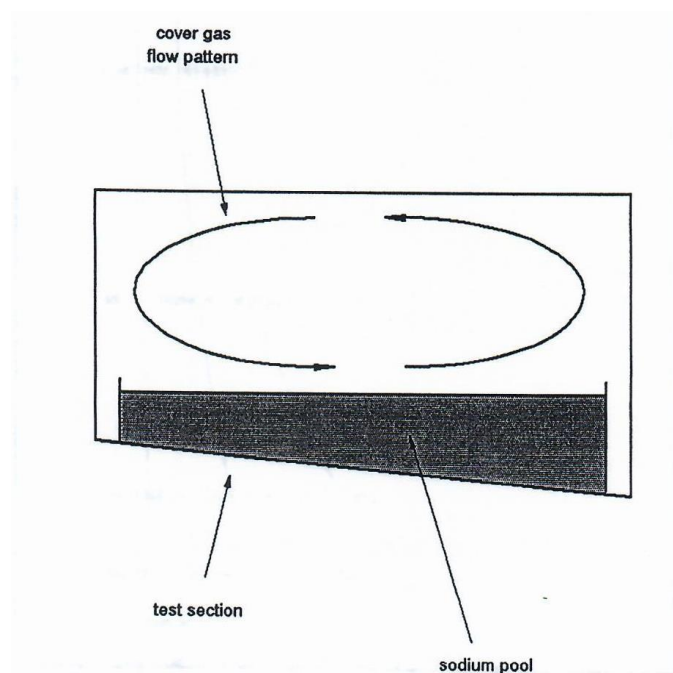


Figure 36: Cover gas circulation pattern

9.6 Further Experimental Studies

In order to extend the earlier work of Anderson [7] to roof temperatures of 160°C and 200°C, the MUSAC test facility had to be modified. Then, further experiments were performed by An [5] during 1990 and 1991. The final version of the liquid sodium test facility in 1990 is shown in Plate 4.

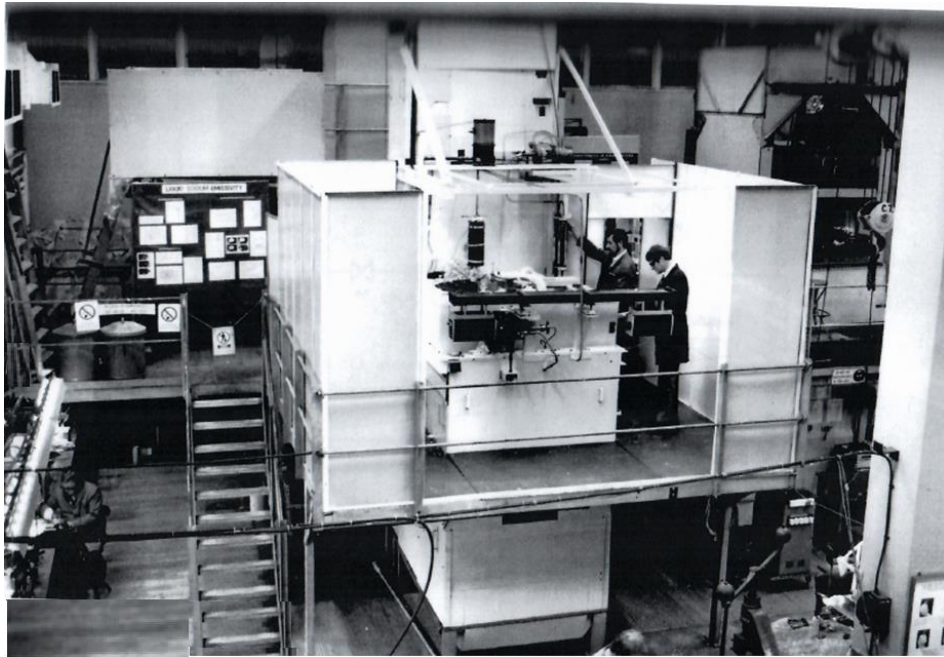


Plate 4: The final version of the liquid sodium test facility in 1990

After An [5] took over the test facility from Anderson [7], he designed an improved forced flow air cooling system. This was then constructed as an alternative means of cooling the roof and obtaining the total rate of heat transfer employed (see Figure 37).

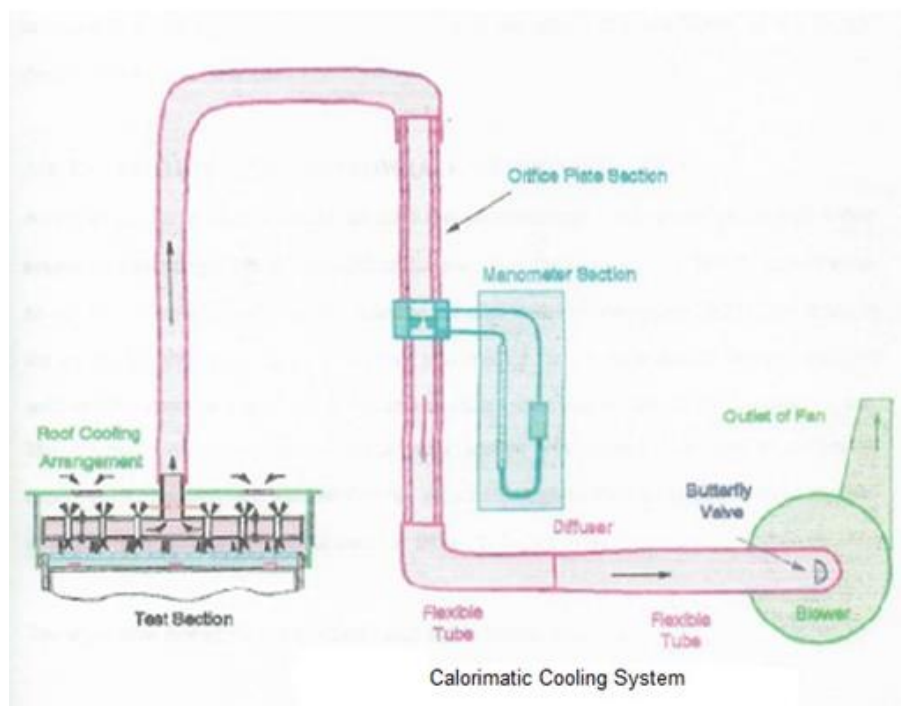


Figure 37: Calorimetric flow cooling section

Thirty-six tubes of 25 mm in diameter penetrate the middle space. Air was induced through the system by the centrifugal blower and was drawn from the surroundings above the rig into the top space and through the tubes from which jets of air emerged and impinged on the top plate of the lower arrangement. The air was drawn into the middle space through holes and then

through the extraction tube which contained baffles to cause mixing to take place and produce a uniform air temperature at the outlet. The temperature rise between inlet and outlet was sensed by a differential thermopile arrangement. A centrifugal blower extracted air from the calorimetric air cooling section through a duct system incorporating an orifice plate flow metering section. The air flow rate could be adjusted using a butterfly valve situated at the inlet to the blower. Inspection of the internal surfaces of the sodium pool test section was made possible later by the installation of a borescope which could be inserted into the rig through an adaptor attached to the sapphire window port on the side wall.

The calorimetric air cooling section had to be installed on the top of the test section roof when experiments using this method of roof heat transfer measurement were performed.

Throughout each test using the calorimetric cooling section, the flow rate had to be carefully adjusted to enable the required roof temperature to be obtained. This was achieved using the butterfly valve at inlet to the centrifugal blower.

9.6.1 Aerosol characteristics

(a) Mass concentration

Before the experiments with roof temperatures of 160°C and 200°C were commenced, some repeat measurements of sodium aerosol characteristics were conducted by An [5] with a 120°C roof temperature as a check on the experimental procedures and also on the state of the test section. The results agreed well with those from the earlier experiments.

After these validation tests had been completed, a series of the measurements with a 160°C roof temperature were carried out, followed by a series of measurements with a 200°C roof temperature.

Aerosol mass concentration results measured as a function of pool temperature using the Malvern Instrument and the Jet Impactor, are shown in Figure 38. The earlier data obtained for 120°C roof temperature are also shown on this figure.

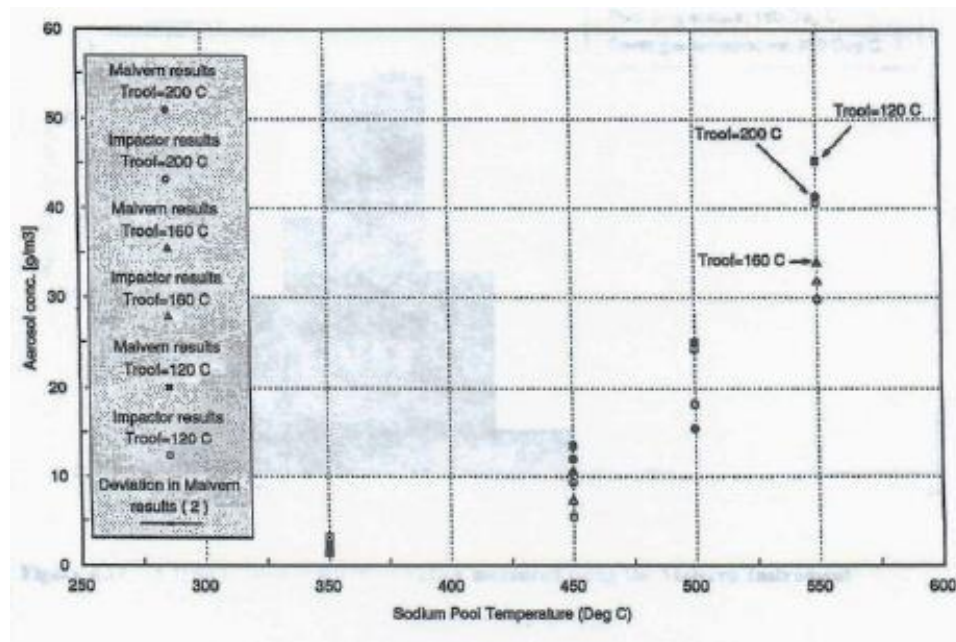


**Figure 38: Summary of aerosol concentration
(roof temperatures: 120°C, 160°C and 200°C)**

It can be seen that the Jet Impactor results were always slightly lower than the Malvern results. The aerosol concentration increases with the sodium pool temperature. There is no systematic influence of the increase in roof temperature on aerosol concentration for a fixed sodium pool temperature over the range of conditions covered.

(b) Aerosol size distribution

A typical volumetric size distribution measured using the Malvern Instrument is shown on Figure 39. This shows that the aerosol size is concentrated in a narrow band, from 5 microns to 25 microns for the particular case shown (sodium pool temperature 550°C, roof temperature 160°C and cover gas temperature 330°C).

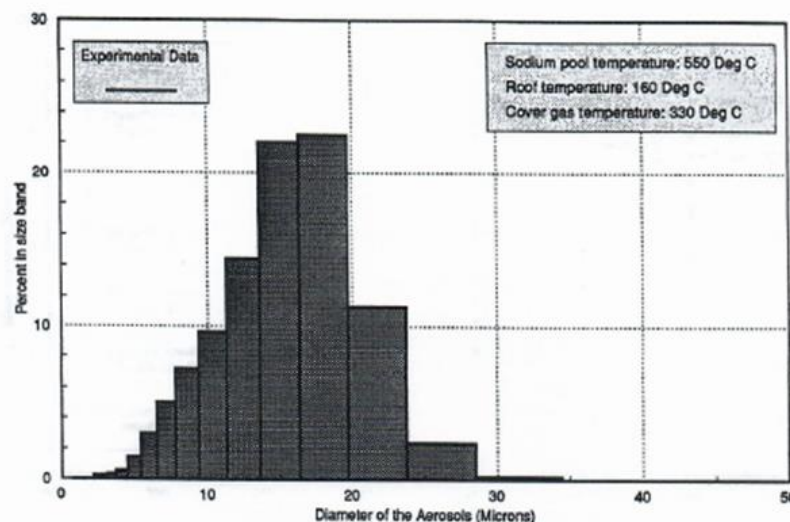


Figure 39: A typical aerosol size distribution measured using the Malvern Instrument

A summary of the 50% volumetric mean diameter (defined such that aerosols with diameters smaller than this value constitute 50% of the total volume of liquid sodium present) as a function of the sodium pool and different roof temperatures is shown on Figure 40. The earlier results for 120°C roof temperature are also plotted on that figure. The value of the mean diameter measured by the Jet Impactor can be seen to be generally low. A small systematic increase in the mean diameter with the increase of roof temperature is evident.

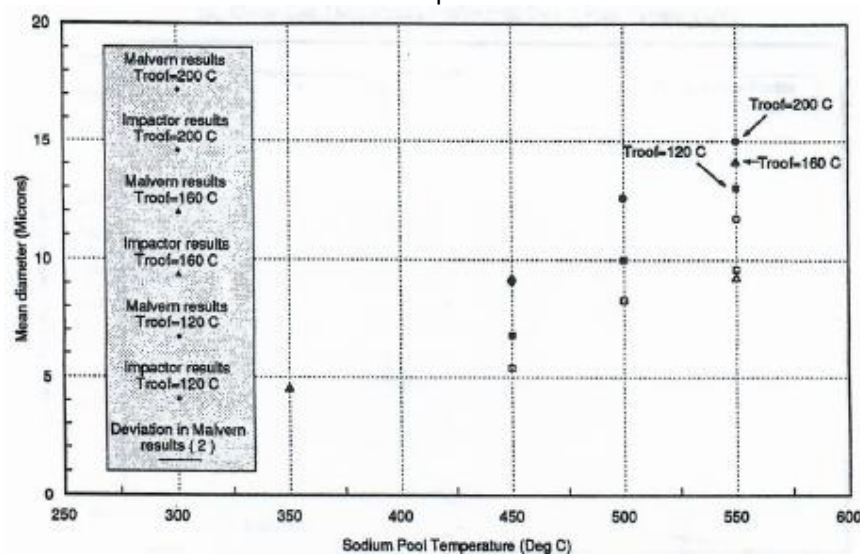


Figure 40: Summary of 50% mean diameter measurements (roof temperatures: 120°C, 160°C and 200°C)

9.6.2 Measurements of cover gas temperature profiles

As part of this further study, temperature profiles in the cover gas were measured using the moveable thermocouple comb for a pool temperature of 550°C and two roof temperature conditions: 160°C and 200°C. Similar measurements were made earlier for a roof temperature of 120°C (Section 9.5.2). Typical results are shown in Figure 41. The temperatures were measured as the comb was moved gradually downwards or upwards in steps.

The temperature profiles measured in these experiments were similar in form to those obtained earlier with a roof temperature of 120°C. The main feature of the temperature profiles is again that most of the temperature change occurred within layers of the cover gas near the pool surface and near the roof. Near the side wall the profiles are only slightly different to these in the centre. The temperature was quite uniform across most of the cover gas space.

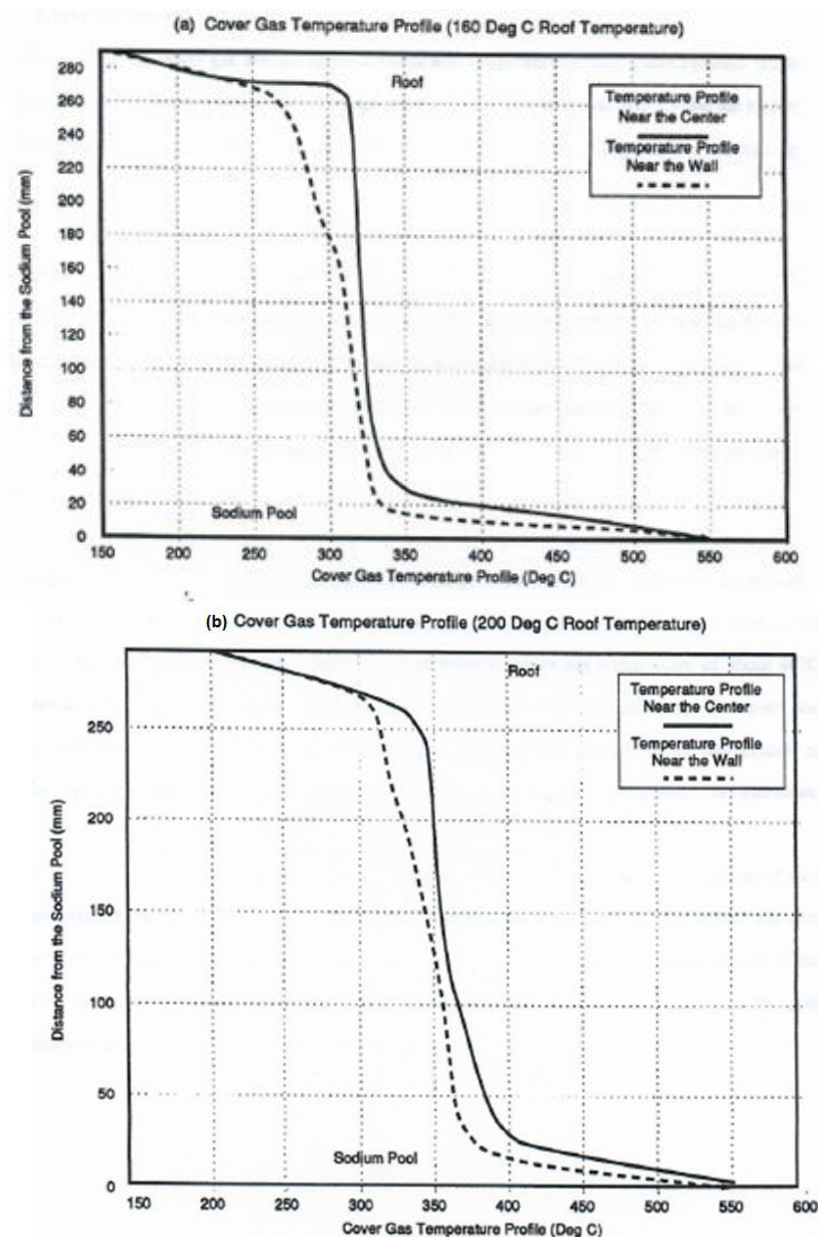


Figure 41: Cover gas temperature profiles measured for roof temperatures of 160°C and 200°C

The measurements needed in order to determine the rate of heat transfer to the roof were synchronised with measurements made using the heat flux sensors. From the heat flux measurements made, it would appear that under normal operation of the test facility the convective flow of cover gas rises above the deep end of the pool and descends above the shallow end. The roof heat fluxes measured by sensors at the deep end were generally higher than those at the shallow end.

Figure 42 shows the heat fluxes measured using the heat flux sensor which is near the centre, compared with the average of the heat flux measurements. Although for low sodium pool temperatures the difference between them is small, with elevated sodium pool temperature, the heat flux in the centre was systematically lower than that of the mid-radius position. This could have resulted from the shielding effect of sodium aerosols in the cover gas on the thermal radiation to the roof.

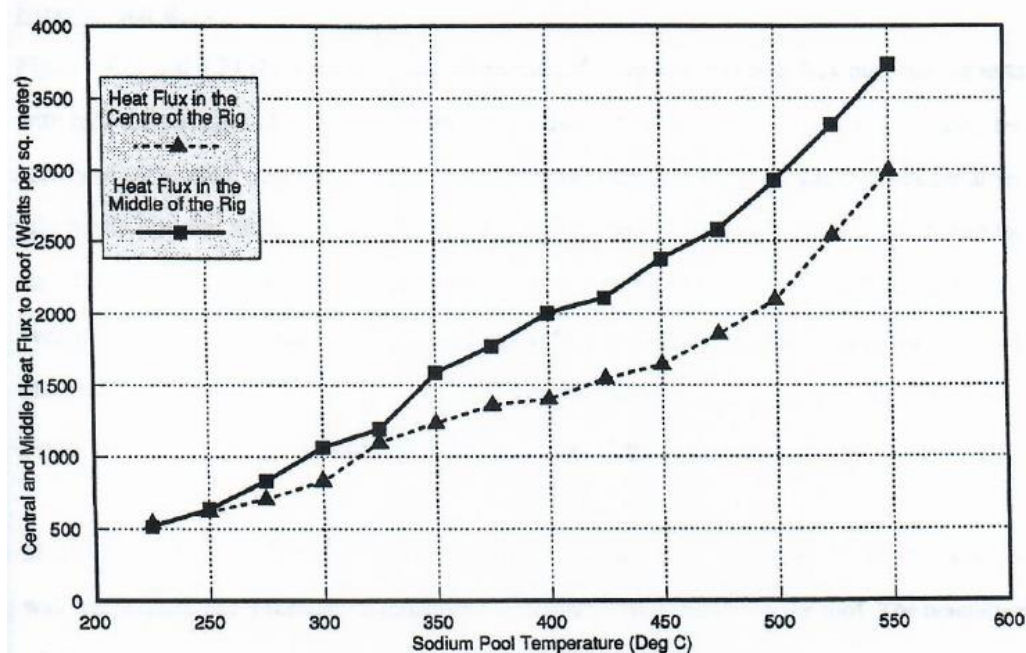


Figure 42: Measured heat flux at the centre and at the mid-radius position as a function of sodium pool temperature

On completion of this evaluation exercise, a programme of work was embarked upon to study the rate of heat transfer to the roof under a variety of operational conditions. In these tests the roof temperature was maintained at one of the three particular temperature conditions: 120°C, 160°C and 200°C and the pool temperature was varied from 300°C to 550°C.

For a fixed roof temperature, a number of tests were made with the sodium pool set at various temperatures. In each case the wall temperature was adjusted to be equal to that of the cover gas. Thus, the rate of heat transfer to the roof was obtained as a function of the pool temperature for a particular roof temperature. For some temperature conditions, a number of nominally identical tests were conducted with a view to testing the repeatability of the measurements and this was found to be very satisfactory. The results of the repeat tests were averaged and deviations were established. These were well within the error band which can be calculated on the basis of all of the sources of uncertainty considered.

Summaries of the roof heat transfer measurements are presented in Figure 43, Figure 44 and Figure 45 for roof temperatures of 120°C, 160°C and 200°C respectively. Data points on these graphs are in each case the average values from the results of several identical repeated

experiments. In Figure 43 (roof temperature: 120°C) the roof heat flux value at 550°C pool temperature is an extrapolated value arrived at on the basis of the measurements at 475°C and 500°C pool temperature. This is because with the calorimetric cooling arrangement in place, it was not possible to perform experiments with the pool temperature above 500°C.

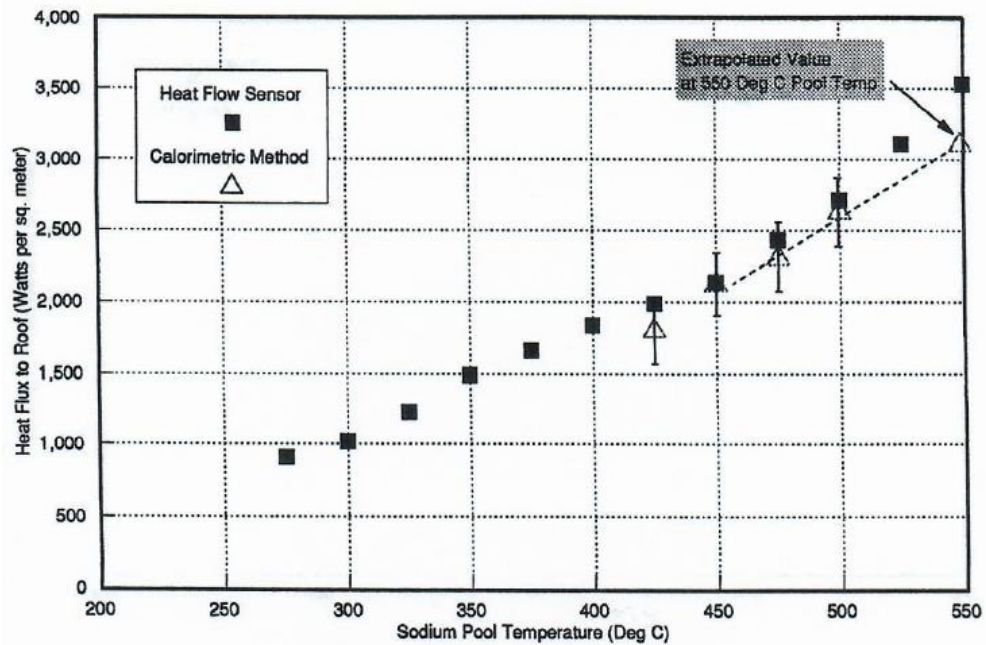


Figure 43: Rate of heat transfer to the roof for a roof temperature of 120°C (temperature of the side wall nominally the same as that of cover gas)

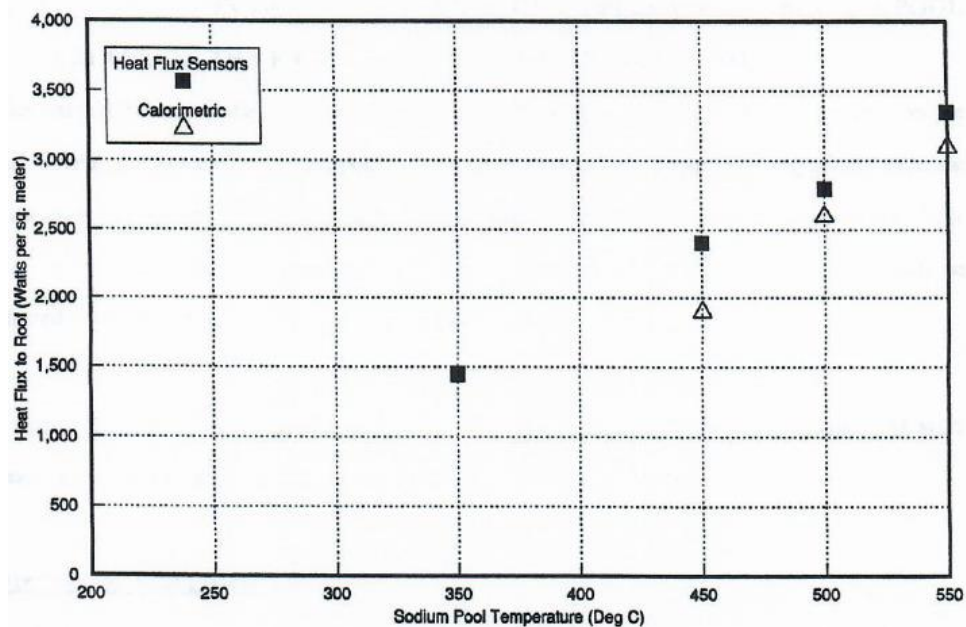


Figure 44: Rate of heat transfer to the roof for a roof temperature of 160°C (temperature of the side wall nominally the same as that of cover gas)

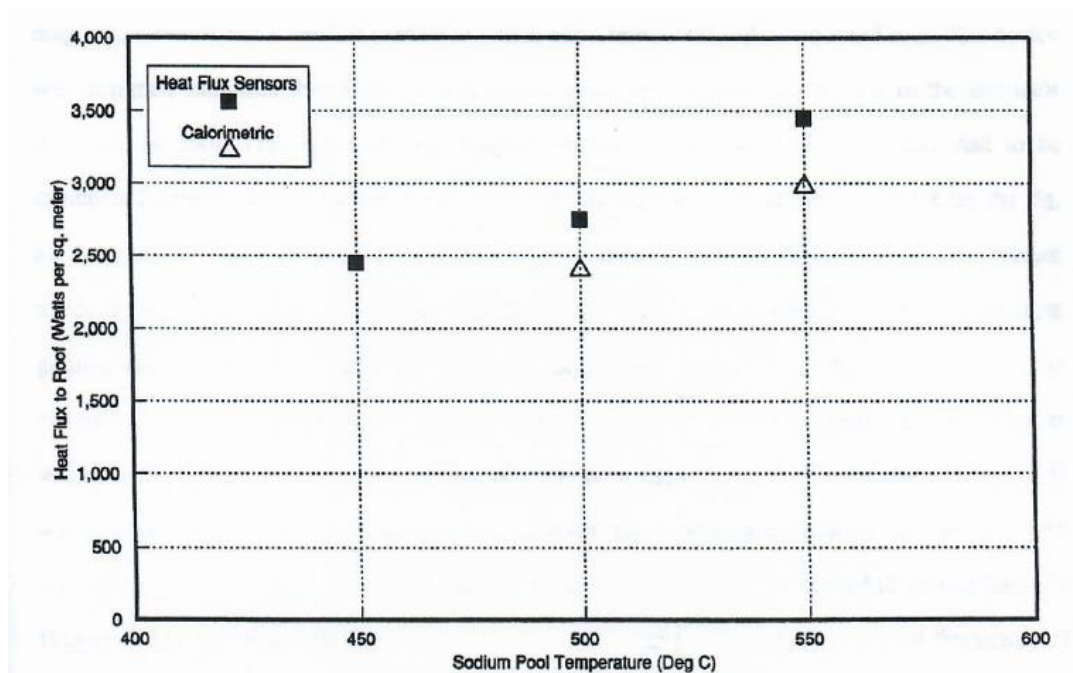


Figure 45: Rate of heat transfer to the roof for a roof temperature of 200°C (temperature of the wall nominally the same as that of cover gas)

For all three roof temperature conditions, it can be seen that for a fixed roof temperature the rate of heat transfer to the roof measured by each of the methods increases steadily with the increase of the pool temperature. An increase in sodium pool temperature results in an increase in the temperature difference between the pool and the roof and consequently in an increase in the temperature of the cover gas and the side wall. This leads to an increase in convective and radiative heat transfer to the roof.

It is perhaps surprising that only a small effect on heat transfer was evident on changing the roof temperature from 120°C to 200°C. As an example, for a pool temperature of 550°C, the rates of heat transfer to the roof measured by the calorimetric method for 120°C, 160°C and 200°C roof temperature are 3100 W/m², 3050 W/m² and 2950 W/m² respectively. Taking into the account the basic uncertainty in the measurements, the variation of these values is well within the uncertainty band. It appears from these experiments that the influence on heat transfer of reducing the driving temperature difference from the pool to the roof by 80°C is counteracted by the increased radiant heat transfer from the side wall to the roof due to the temperature of the wall being kept higher by about 40°C due to the wall temperature being kept equal to the cover gas temperature.

After operation many times at higher roof temperature conditions (160°C and 200°C), the rig was operated again from time to time at the lowest roof temperature (120°C). It was found that the roof heat transfer measurements for such tests repeated the corresponding earlier experimental results extremely well. Visual observations revealed that there was no definite change in the appearance of the internal surfaces of the test facility. This confirms the conclusion that the radiative properties of the internal surfaces were not changing.

9.7 Conclusions

On the basis of the measurements made in the course of the further programme of experiments (with the roof at temperatures of 120°C, 160°C and 200°C) and the initial experiments (with the roof at a temperature of 120°C), the following conclusions can be drawn:

- ▶ The rate of heat transfer to the roof increases monotonically with increase of the sodium pool temperature for fixed roof temperature. For the temperature conditions covered in the present series of tests (roof temperatures: 120°C, 160°C and 200°C; pool temperature: 300°C to 550°C), the effect of changing roof temperature on the rate of heat transfer to the roof for fixed pool temperature is small. At a pool temperature of 550°C, the measured heat flux to the roof was 3500 W/m² as found by integration of the heat flux sensor measurements and 3000 W/m² as measured by the calorimetric method.
- ▶ Over the range of experimental conditions covered in the experiments, the cover gas space is well mixed. Consequently, the bulk of the cover gas space is at a quite uniform temperature and the sodium aerosol characteristics are likely to be uniform. Experiments made earlier have demonstrated that varying the sampling positions in the cover gas region did not systematically change the measured sodium aerosol characteristics. Thus, the aerosol characteristics measured should be representative of the whole cover gas space.
- ▶ In the roof temperature range from 120°C to 200°C, change of the roof temperature does not appear to have any systematic influence on the sodium aerosol concentration. For a fixed pool temperature this change in roof temperature resulted in an increase in cover gas temperature of about 40°C (because the wall temperature was kept equal to the cover gas temperature). The controlling parameter governing the sodium aerosol concentration seems to be the temperature of the liquid sodium pool.
- ▶ There does seem to be a slight systematic change in aerosol mean diameter with increase of roof temperature but the effect is small. In the roof temperature range covered, the higher the roof temperature, the larger is the 50% volumetric mean diameter of the sodium aerosols. The pool temperature has a much stronger influence on this characteristic of the aerosols. The higher the pool temperature, the larger is the mean aerosol diameter.

At this stage of the investigation in 1993, research at the University of Manchester on sodium-cooled fast reactors came to an abrupt end when the UK Government suddenly decided to cease funding research and development on such reactors. The Nuclear Engineering Research Group at Manchester had to de-commission all of its Liquid Sodium Research Facilities and take advantage of an offer from the UKAEA Risley Laboratories to decontaminate and scrap all of its sodium-contaminated equipment.

10 References

- [1] Tong, D.K.W., Sodium pool emittance, PhD thesis, University of Manchester, UK, 1985.
- [2] Romero, E., Enhancement of the emittance of radiating surfaces with application to nuclear plant, PhD thesis, University of Manchester, UK, 1986.
- [3] Iravanian, L., Measurements of the emissivity of sodium-contaminated stainless steel surfaces, MSc thesis, University of Manchester, UK, 1985.
- [4] Lam, K.L.A., Measurements of the emissivity of stainless steel surfaces promoting condensation and evaporation of sodium with application to fast reactors, PhD thesis, University of Manchester, UK, 1988.
- [5] An, P., Studies of basic phenomena involved in radiative heat transfer within the cover gas region of sodium cooled fast breeder reactors, PhD thesis, University of Manchester, UK, 1992.
- [6] Burns, R.A., Heat transfer studies with application to nuclear reactors, PhD thesis, University of Manchester, UK, 1989.
- [7] Anderson, A., Studies of aerosol characteristics, heat transfer and mass transfer with application to the cover gas region of sodium cooled fast reactors, PhD thesis, University of Manchester, UK, 1991.

DOCUMENT INFORMATION

Project : Project FORTE - Nuclear Thermal Hydraulics Research & Development
Report Title : University of Manchester Research on the Aerosol-Laden Argon Cover Gas Region above the Sodium Pool of an LMFBR
Client : Department for Business, Energy and Industrial Strategy (BEIS)

Report No. : FNC 53798/48652R	Compiled By : Professor J D Jackson (University of Sheffield)
Issue No. : 1	Verified By : Professor S. He (University of Sheffield)
Date : August 2019	Approved By : R. Underhill

Legal Statement

This document has been prepared for the UK Government Department for Business, Energy and Industrial Strategy (BEIS) by Frazer-Nash Consultancy Ltd, and any statements contained herein referring to 'we' or 'our' shall apply to Frazer-Nash Consultancy and BEIS both individually and jointly.

The Copyright in this work is vested in Frazer-Nash Consultancy Limited. Reproduction in whole or in part or use for tendering or manufacturing purposes is prohibited except under an agreement with or with the written consent of Frazer-Nash Consultancy Limited and then only on the condition that this notice is included in any such reproduction.

This document is provided for general information only. It is not intended to amount to advice or suggestions on which any party should, or can, rely. You must obtain professional or specialist advice before taking or refraining from taking any action on the basis of the content of this document.

We make no representations and give no warranties or guarantees, whether express or implied, that the content of this document is accurate, complete, up to date, free from any third party encumbrances or fit for any particular purpose. We disclaim to the maximum extent permissible and accept no responsibility for the consequences of this document being relied upon by you, any other party or parties, or being used for any purpose, or containing any error or omission.

Except for death or personal injury caused by our negligence or any other liability which may not be excluded by an applicable law, we will not be liable to any party placing any form of reliance on the document for any loss or damage, whether in contract, tort (including negligence) breach of statutory duty, or otherwise, even if foreseeable, arising under or in connection with use of or reliance on any content of this document in whole or in part.

This document represents the views of Frazer-Nash Consultancy Limited and does not represent the views of BEIS or the UK Government more widely.

Originating Office: FRAZER-NASH CONSULTANCY LIMITED
The Cube, 1 Lower Lamb Street, Bristol, BS1 5UD
T: +44 (0)117 9226242 F: +44 (0)117 9468924 W: www.fnc.co.uk



Frazer-Nash Consultancy Ltd

The Cube
1 Lower Lamb Street
Bristol
BS1 5UD

T +44 (0)117 9226242
F +44 (0)117 9468924

www.fnc.co.uk

Offices at:
Bristol, Burton-on-Trent, Dorchester,
Dorking, Glasgow, Plymouth, Warrington
and Adelaide